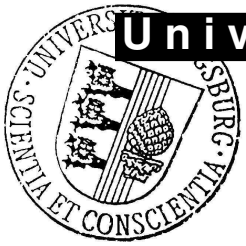

Universität Augsburg

Institut für
Mathematik

Johanna Kerler-Back, Tatjana Stykel

Model Order Reduction for Magneto-Quasistatic Equations

Preprint Nr. 14/2015 — 23. Oktober 2015

Institut für Mathematik, Universitätsstraße, D-86135 Augsburg http://www.math.uni-augsburg.de/

Impressum:

Herausgeber:

Institut für Mathematik
Universität Augsburg
86135 Augsburg
`http://www.math.uni-augsburg.de/de/forschung/preprints.html`

ViSdP:

Tatjana Stykel
Institut für Mathematik
Universität Augsburg
86135 Augsburg

MODEL ORDER REDUCTION FOR MAGNETO-QUASISTATIC EQUATIONS

JOHANNA KERLER-BACK† AND TATJANA STYKEL†

Abstract. We consider model reduction of Maxwell's equations arising in magneto-quasistatic field problems. A finite element discretization of such equations leads to large-scale differential-algebraic equations of special structure. For model reduction of linear systems, we employ a balanced truncation approach, whereas nonlinear systems are reduced using a proper orthogonal decomposition method combined with a discrete empirical interpolation technique. We will exploit the special structure of the underlying problem to improve the performance of the model reduction algorithms. Furthermore, we discuss an efficient evaluation of the Jacobi matrix required in nonlinear time integration of the reduced models.

Key words. Maxwell's equations, magneto-quasistatic problems, model order reduction, balanced truncation, proper orthogonal decomposition, discrete empirical interpolation method

AMS subject classifications. 34A09, 35Q61, 37M99, 65F30, 93A15

1. Magneto-quasistatic simulation. Nowadays, integrated circuits play an increasingly important role. Modelling of electromagnetic effects in high-frequency and high-speed electronic systems leads to coupled electromagnetic-circuit models of high complexity. The development of efficient, fast and accurate simulation tools for such models is of great importance in the computer-aided design of electromagnetic structures offering significant savings in production cost and time.

Let $\Omega \subset \mathbb{R}^d$, $d = 2, 3$, be a bounded domain which is composed of the conducting and non-conducting subdomains Ω_1 and Ω_2 such that $\bar{\Omega} = \bar{\Omega}_1 \cup \bar{\Omega}_2$. In magneto-quasistatic (MQS) problems, the contribution of the displacement currents is negligible compared to the conductive currents. Then the magnetic field can be described by Maxwell's equations in magnetic vector potential formulation

$$\begin{aligned} \sigma\frac{\partial A}{\partial t} + \nabla \times \big(\nu(\|\nabla \times A\|^2)\nabla \times A\big) &= J, && \text{in } \Omega \times (0,T), \\ A \times n_o &= 0, && \text{on } \partial\Omega \times (0,T), \\ A(\cdot,0) &= A_0, && \text{in } \Omega, \end{aligned} \tag{1.1}$$

where $A : \bar{\Omega} \times (0,T) \to \mathbb{R}^d$ is the magnetic vector potential, $\nu : \Omega \times \mathbb{R}_0^+ \to \mathbb{R}^+$ is the magnetic reluctivity, $\sigma : \Omega \to \mathbb{R}_0^+$ is the electric conductivity vanishing on Ω_2, n_o is the outer unit normal vector to the boundary $\partial\Omega$ of Ω, and $J : \Omega \times (0,T) \to \mathbb{R}^d$ is the current density applied by external sources. For a conductor model with m stranded conductors, the source function has the form

$$J = \chi_{\mathrm{str}}\iota,$$

where $\chi_{\mathrm{str}} : \Omega \to \mathbb{R}^{d,m}$ is a divergence-free winding function and $\iota : [0,T] \to \mathbb{R}^m$ is the electrical current in the conductors [37]. A relation between the current ι and the voltage $u : [0,T] \to \mathbb{R}^m$ is given by Faraday's law of induction

$$\int_\Omega \chi_{\mathrm{str}}^T \frac{\partial}{\partial t} A \, d\xi + R\,\iota = u, \tag{1.2}$$

†Institut für Mathematik, Universität Augsburg, Universitätsstraße 14, 86159 Augsburg, Germany (kerler@math.uni-augsburg.de, stykel@math.uni-augsburg.de) Supported by the Research Network KoSMos: *Model reduction based simulation of coupled PDAE systems* funded by the German Ministry of Education and Science (BMBF), grant 05M13WAA.

‡Version January 10, 2017

where $R \in \mathbb{R}^{m,m}$ is the resistance matrix which is symmetric and positive definite.

Unfortunately, the numerical solution of the MQS systems requires an enormous amount of storage and large computational time. To reduce numerical effort, model order reduction can be used. The goal of model reduction is to replace a large-scale system by a reduced-order model which captures the dynamic behaviour of the original system, preserves its essential physical properties and requires much less simulation time.

Model reduction of electromagnetic problems is currently a very active research area because faster simulations are essential in parameter study and computational optimization of electromagnetic structures. Model reduction of time-harmonic Maxwell's equations based on Krylov subspace methods has been considered in [8, 9, 47]. For model reduction of linear MQS systems, proper orthogonal decomposition (POD) has been used in [31, 35]. This method was originally developed for the approximation of turbulent structures [38] and then applied to many practical problems including also nonlinear MQS field simulation [17, 18, 34]. Furthermore, in [3, 12, 33], a reduced basis method has been used to reduce the dimension of parametric electromagnetic systems.

In this paper, we consider model reduction of the MQS system (1.1), (1.2). A spatial discretization of such a system using the finite integration technique (FIT) [45] or the finite element method (FEM), e.g., [27] leads to a system of differential-algebraic equations (DAEs), where the algebraic constraints occur due to the presence of the non-conducting subdomain. We will exploit the special structure of the semidiscretized MQS system to construct the efficient model reduction methods for linear and nonlinear problems.

The paper is organized as follows. In Section 2, we consider the FEM discretization of the MQS system (1.1), (1.2). In Section 3, we discuss model order reduction of linear MQS systems using balanced truncation. Section 4 deals with model reduction of nonlinear MQS systems using proper orthogonal decomposition combined with a discrete empirical interpolation method (DEIM) [11]. We also propose an efficient implementation of the matrix DEIM [46] for the approximation of the Jacobian. Unlike the sparse matrix approximation strategy in [39], our approach avoids the vectorization of the matrix snapshots and does not rely on their sparsity. Finally, in Section 5, we present some results of numerical experiments for a single-phase transformer model.

2. Finite element discretization. In this section, we consider the finite element discretization (FEM) of the MQS system (1.1), (1.2) and study the properties of the discretized system. Assume that the electrical conductivity and the magnetic reluctivity have different structure in the conducting and non-conducting subdomains

$$\sigma(\xi) = \begin{cases} \sigma_1 > 0 & \text{for } \xi \in \Omega_1 \\ 0 & \text{for } \xi \in \Omega_2 \end{cases}, \qquad \nu(\xi,\eta) = \begin{cases} \nu_1(\eta) & \text{for } \xi \in \Omega_1 \\ \nu_2 > 0 & \text{for } \xi \in \Omega_2 \end{cases},$$

where $\nu_1 : \mathbb{R}_0^+ \to \mathbb{R}^+$. The weak formulation of (1.1) leads to the variational equation

$$\int_\Omega \sigma \frac{\partial}{\partial t} A \cdot \varphi \, d\xi + \int_\Omega \nu(\|\nabla \times A\|^2)(\nabla \times A) \cdot (\nabla \times \varphi) \, d\xi = \int_\Omega \chi_{\mathrm{str}} \iota \cdot \varphi \, d\xi \tag{2.1}$$

for all $\varphi \in H_0(\mathrm{curl}, \Omega)$ and almost everywhere on (0,T). Here,

$$\begin{aligned} H_0(\mathrm{curl}, \Omega) &= \{ \phi \in H(\mathrm{curl}, \Omega) \ : \ \phi \times n = 0 \text{ on } \partial\Omega \}, \\ H(\mathrm{curl}, \Omega) &= \{ \phi \in L_2(\Omega)^d \ : \ \mathrm{curl}\, \phi \in L_2(\Omega)^d \}. \end{aligned}$$

The existence of a weak solution to (1.1), (1.2) with $\nu_1(\eta) \equiv \nu_1 > 0$ has been investigated in [30], whereas the nonlinear 2D case has been considered in [21].

For the FEM discretization of the MQS system (1.1), (1.2), we use the $H(\mathrm{curl}, \Omega)$-conforming Nédélec elements [29] and approximate the magnetic vector potential $A(\xi, t)$ by a linear combination

$$A(\xi, t) \approx \sum_{k=1}^{n_a} \alpha_k(t) \varphi_k(\xi),$$

where φ_k are the edge shape functions which are continuous inside the elements and tangentially continuous at the element interfaces. The standard Galerkin projection yields a nonlinear system of DAEs

$$\begin{aligned} \mathcal{E}\, \dot{x} &= \mathcal{A}(x) x + \mathcal{B}\, u, \\ y &= \mathcal{C}\, x \end{aligned} \tag{2.2}$$

with the state vector $x = [a^T, \iota^T]^T$, the control u, the output $y = \iota$, and

$$\mathcal{E} = \begin{bmatrix} M & 0 \\ X^T & 0 \end{bmatrix}, \quad \mathcal{A}(x) = \begin{bmatrix} -K(a) & X \\ 0 & -R \end{bmatrix}, \quad \mathcal{B} = \mathcal{C}^T = \begin{bmatrix} 0 \\ I \end{bmatrix}. \tag{2.3}$$

Here, $a = [\alpha_1, \ldots, \alpha_{n_a}]^T$ is a semidiscretized vector of magnetic potentials, M is a conductivity matrix, $K(a)$ is a curl-curl matrix, and X is a coupling matrix with the entries

$$\begin{aligned} (M)_{kl} &= \int_\Omega \sigma \varphi_l \cdot \varphi_k \, d\xi, \quad k, l = 1, \ldots, n_a, \\ (K(a))_{kl} &= \int_\Omega \nu(\|\nabla \times \sum_{j=1}^{n_a} \alpha_j \varphi_j\|^2)(\nabla \times \varphi_l) \cdot (\nabla \times \varphi_k) \, d\xi, \quad k, l = 1, \ldots, n_a, \\ (X)_{kl} &= \int_\Omega \chi_{\mathrm{str},l} \cdot \varphi_k \, d\xi, \quad k = 1, \ldots, n_a, \ l = 1, \ldots, m, \end{aligned}$$

respectively, where $\chi_{\mathrm{str},l}$ denotes the l-th column of χ_{str}. Clearly, M and $K(a)$ are both symmetric. Reordering the state variables accordingly to the conducting and non-conducting subdomains Ω_1 and Ω_2, we can partition the vector a and the matrices M, $K(a)$ and X as

$$a = \begin{bmatrix} a_1 \\ a_2 \end{bmatrix}, \ M = \begin{bmatrix} M_{11} & 0 \\ 0 & 0 \end{bmatrix}, \ K(a) = \begin{bmatrix} K_{11}(a) & K_{12} \\ K_{21} & K_{22} \end{bmatrix}, \ X = \begin{bmatrix} X_1 \\ X_2 \end{bmatrix}, \tag{2.4}$$

where $a_1 \in \mathbb{R}^{n_1}$, $a_2 \in \mathbb{R}^{n_2}$, $M_{11} \in \mathbb{R}^{n_1, n_1}$ is symmetric, positive definite, the matrices $K_{12} \in \mathbb{R}^{n_1, n_2}$, $K_{21} = K_{12}^T \in \mathbb{R}^{n_2, n_1}$ and $K_{22} \in \mathbb{R}^{n_2, n_2}$ are constant, $X_1 \in \mathbb{R}^{n_1, m}$, and $X_2 \in \mathbb{R}^{n_2, m}$. Without loss of generality we may assume that K_{22} is positive definite. In the 2D case, this condition is fulfilled, since the curl-curl matrix $K(a)$ is positive definite. For 3D problems, the positive definiteness of K_{22} can always be achieved by gauging [19, 25]. Moreover, we assume that

$$\begin{aligned} &\mathrm{supp}(\chi_{\mathrm{str},i}) \cap \Omega_2 \neq \emptyset \quad \text{for } i = 1, \ldots, m, \\ &\mathrm{supp}(\chi_{\mathrm{str},i}) \cap \mathrm{supp}(\chi_{\mathrm{str},j}) = \emptyset \quad \text{for } i \neq j. \end{aligned}$$

The first condition means that the coupling is not only on the conductive part. This condition together with the second one implies that the coupling matrix X_2 has full column rank. We will exploit this property to establish the index of the DAE (2.2).

For DAEs, several index concepts have been introduced in the literature, e.g., [10, 22, 23], see also [26] for a recent survey. Here, we analyze the tractability index from [23] which is defined for the nonlinear DAE (2.2) as follows. Let $h(x) = \mathcal{A}(x)x$ and let $J_h(x)$ denote the Jacobi matrix of h at x. Consider a matrix chain

$$\begin{aligned} \mathcal{G}_0 &= \mathcal{E}, & \mathcal{H}_0 &= J_h, \\ \mathcal{G}_j &= \mathcal{G}_{j-1} - \mathcal{H}_{j-1}\mathcal{Q}_{j-1}, & \mathcal{H}_j &= \mathcal{H}_{j-1}(I - \mathcal{Q}_{j-1}), \end{aligned}$$

where $\mathcal{Q}_j$ is a projector onto $\ker \mathcal{G}_j$. System (2.2) has the tractability index k if the matrix $\mathcal{G}_k$ is nonsingular. Note that the defined index does not depend on the choice of the projectors $\mathcal{Q}_j$. The following theorem establishes that system (2.2) has the tractability index one. A similar result for the FIT-discretized model is obtained in [2].

THEOREM 2.1. *Consider the DAE* (2.2)*, where M_{11} and K_{22} are symmetric, positive definite and X_2 has full column rank. Then this system has the tractability index one.*

Proof. Let the columns of $Y \in \mathbb{R}^{n_2, n_2-m}$ form an orthonormal basis of $\ker X_2^T$. Then the projector $\mathcal{Q}_0$ onto $\ker \mathcal{G}_0 = \ker \mathcal{E}$ can be chosen as

$$\mathcal{Q}_0 = \begin{bmatrix} 0 & 0 & 0 \\ 0 & YY^T & 0 \\ 0 & 0 & I \end{bmatrix}.$$

We have

$$\mathcal{G}_1 = \mathcal{G}_0 - \mathcal{H}_0\mathcal{Q}_0 = \begin{bmatrix} M_{11} & K_{12}YY^T & -X_1 \\ 0 & K_{22}YY^T & -X_2 \\ X_1^T & X_2^T & R \end{bmatrix}.$$

Assume that there exists a vector $v = [v_1^T, v_2^T, v_3^T]^T$ such that $\mathcal{G}_1 v = 0$. Then

$$M_{11}v_1 + K_{12}YY^Tv_2 - X_1v_3 = 0, \tag{2.5}$$
$$+ K_{22}YY^Tv_2 - X_2v_3 = 0, \tag{2.6}$$
$$X_1^Tv_1 + \quad X_2^Tv_2 + Rv_3 = 0. \tag{2.7}$$

Multiplying equation (2.6) from the left with Y^T, we obtain that $Y^TK_{22}YY^Tv_2 = 0$. Since K_{22} is symmetric, positive definite, then $Y^TK_{22}Y$ is nonsingular, and, hence, $Y^Tv_2 = 0$. In this case, equation (2.6) implies that $X_2v_3 = 0$. Since X_2 has full column rank, we have $v_3 = 0$. Then taking into account that M_{11} is nonsingular, we get from equation (2.5) that $v_1 = 0$. Finally, equation (2.7) implies that $X_2^Tv_2 = 0$. Therefore, there exist $w \in \mathbb{R}^{n_2-m}$ such that $v_2 = Yw$. Multiplying this equation from the left with Y^T, we obtain $0 = Y^Tv_2 = Y^TYw = w$, and, hence $v_2 = 0$. Thus, the matrix $\mathcal{G}_1$ is nonsingular and system (2.2) has the tractability index one. ∎

2.1. ODE formulation. Using the basis matrix Y as in the proof of Theorem 2.1, we can transform the DAE system (2.2) into a system of ordinary differential equations (ODEs)

$$E_1\dot{x}_1 = A_1(x_1)x_1 + B_1u, \tag{2.8a}$$
$$y = C_1x_1, \tag{2.8b}$$

with a nonsingular matrix E_1. Let $Z = X_2(X_2^T X_2)^{-1/2}$. Then $Z^T Z = I$ and $Z^T Y = 0$. Hence, the matrix $[Z, Y]$ is orthogonal. We multiply the first equation in (2.2) from the left with the orthogonal matrix

$$T = \begin{bmatrix} I_{n_1} & 0 & 0 \\ 0 & Z^T & 0 \\ 0 & Y^T & 0 \\ 0 & 0 & I_m \end{bmatrix}, \tag{2.9}$$

where I_k denotes a $k \times k$ identity matrix, and introduce a transformed state vector $Tx = \begin{bmatrix} a_1^T,\ a_{21}^T,\ a_{22}^T,\ \iota^T \end{bmatrix}^T$ partitioned according to T. Then the transformed DAE system can be written as

$$\begin{aligned} M_{11}\dot{a}_1 &= -K_{11}(a_1)a_1 - K_{12}Za_{21} - K_{12}Ya_{22} + X_1\,\iota \\ 0 &= -Z^T K_{21}a_1 - Z^T K_{22}Za_{21} - Z^T K_{22}Ya_{22} + Z^T X_2\,\iota \\ 0 &= -Y^T K_{21}a_1 - Y^T K_{22}Za_{21} - Y^T K_{22}Ya_{22} \\ X_1^T\dot{a}_1 + X_2^T Z\dot{a}_{21} &= -R\,\iota + u. \end{aligned} \tag{2.10}$$

Since $Y^T K_{22} Y$ and R are both nonsingular, we get from the third and fourth equations

$$\begin{aligned} a_{22} &= -(Y^T K_{22}Y)^{-1}Y^T K_{21}a_1 - (Y^T K_{22}Y)^{-1}Y^T K_{22}Za_{21}, \\ \iota &= -R^{-1}X_1^T\dot{a}_1 - R^{-1}X_2^T Z\dot{a}_{21} + R^{-1}u. \end{aligned} \tag{2.11}$$

Substituting these vectors into the first and second equations, we obtain the state equation (2.8a) with $x_1 = \begin{bmatrix} a_1^T,\ a_{21}^T \end{bmatrix}^T \in \mathbb{R}^n$, $n = n_1 + m$, and

$$E_1 = \begin{bmatrix} M_{11} + X_1 R^{-1} X_1^T & X_1 R^{-1} X_2^T Z \\ Z^T X_2 R^{-1} X_1^T & Z^T X_2 R^{-1} X_2^T Z \end{bmatrix}, \tag{2.12a}$$

$$A_1(x_1) = -\begin{bmatrix} K_{11}(a_1) & K_{12}Z \\ Z^T K_{21} & Z^T K_{22} Z \end{bmatrix} + \begin{bmatrix} K_{12} \\ Z^T K_{22} \end{bmatrix} Y \big(Y^T K_{22} Y\big)^{-1} Y^T [\, K_{21},\ K_{22}Z\,], \tag{2.12b}$$

$$B_1 = \begin{bmatrix} X_1 \\ Z^T X_2 \end{bmatrix} R^{-1}. \tag{2.12c}$$

The following lemma shows that E_1 is nonsingular and gives its inverse.

LEMMA 2.2. *Let M_{11} be nonsingular and let X_2 have full column rank. Then the matrix E_1 in* (2.12a) *is nonsingular and its inverse is given by*

$$E_1^{-1} = \begin{bmatrix} M_{11}^{-1} & -M_{11}^{-1}X_1(X_2^T X_2)^{-1/2} \\ -(X_2^T X_2)^{-1/2}X_1^T M_{11}^{-1} & (X_2^T X_2)^{-1/2}\big(R + X_1^T M_{11}^{-1} X_1\big)(X_2^T X_2)^{-1/2} \end{bmatrix}. \tag{2.13}$$

Proof. Using $X_2^T Z = (X_2^T X_2)^{1/2}$ the matrix E_1 can be factorized as

$$E_1 = \begin{bmatrix} M_{11} & X_1 R^{-1}(X_2^T X_2)^{1/2} \\ 0 & (X_2^T X_2)^{1/2} R^{-1} (X_2^T X_2)^{1/2} \end{bmatrix} \begin{bmatrix} I & 0 \\ (X_2^T X_2)^{-1/2} X_1^T & I \end{bmatrix}. \tag{2.14}$$

Since M_{11} and $(X_2^TX_2)^{1/2}R^{-1}(X_2^TX_2)^{1/2}$ are both nonsingular, the matrix E_1 is nonsingular too. The inverse of E_1 has the form

$$\begin{aligned} E_1^{-1} &= \begin{bmatrix} I & 0 \\ -(X_2^TX_2)^{-1/2}X_1^T & I \end{bmatrix} \begin{bmatrix} M_{11}^{-1} & -M_{11}^{-1}X_1(X_2^TX_2)^{-1/2} \\ 0 & (X_2^TX_2)^{-1/2}R(X_2^TX_2)^{-1/2} \end{bmatrix} \\ &= \begin{bmatrix} M_{11}^{-1} & -M_{11}^{-1}X_1(X_2^TX_2)^{-1/2} \\ -(X_2^TX_2)^{-1/2}X_1^TM_{11}^{-1} & (X_2^TX_2)^{-1/2}\big(R+X_1^TM_{11}^{-1}X_1\big)(X_2^TX_2)^{-1/2} \end{bmatrix}. \end{aligned}$$

□

Since E_1 is nonsingular, the output equation in (2.2) can be written using (2.11) and (2.13) as

$$y = \iota = -R^{-1}\left[\,X_1^T,\ X_2^TZ\,\right]E_1^{-1}(A_1(x_1)x_1 + B_1u) + R^{-1}u = C_1x_1 + D_1u$$

with

$$\begin{aligned} C_1 &= -R^{-1}\left[\,X_1^T,\ X_2^TZ\,\right]E_1^{-1}A_1(x_1) \\ &= (X_2^TX_2)^{-1}X_2^T\left(I - K_{22}Y(Y^TK_{22}Y)^{-1}Y^T\right)\left[\,K_{21},\ K_{22}Z\,\right], \\ D_1 &= -R^{-1}\left[\,X_1^T,\ X_2^TZ\,\right]E_1^{-1}B_1 + R^{-1} = 0. \end{aligned} \tag{2.15}$$

Thus, we obtain the ODE system (2.8) with the system matrices as in (2.12) and (2.15). In the following, we will use the ODE formulation to construct the efficient model reduction methods for linear and nonlinear MQS systems.

3. Model reduction of linear MQS systems. In this section, we consider model reduction of the MQS system (2.2), where ν_1 is assumed to be constant in Ω_1. Then the matrix K_{11} in (2.4) does not depend on the semidiscretized potential a, and we obtain a linear time-invariant DAE system

$$\begin{aligned} \mathcal{E}\,\dot{x} &= \mathcal{A}\,x + \mathcal{B}\,u, \\ y &= \mathcal{C}\,x. \end{aligned} \tag{3.1}$$

For model reduction of such a system, we can use balanced truncation as described in [40] which is based on decoupling (3.1) into the slow and fast subsystems and reducing them separately. Thereby, it is essential to ensure that no errors occur in the output of the reduced-order fast subsystem meaning that only uncontrollable and unobservable state components of the fast subsystems can be removed. Violation of these conditions may lead to an inaccurate approximation and physically incorrect results, see [41]. Unfortunately, the model reduction approach from [40] requires the computation of the spectral projectors onto the deflating subspaces of the pencil $\lambda\mathcal{E} - \mathcal{A}$ corresponding to the finite and infinite eigenvalues. Recently, some modifications of this approach avoiding the spectral projectors have been presented in [13, 16, 43] for structured DAE systems including semi-explicit DAEs of index 1, Stokes-type systems of index 2 and mechanical systems of index 1 and 3, see also a recent survey [7]. They all are based on an implicit index reduction and an equivalence between the Schur complement linear systems and systems with the original system matrices. This idea can also be extended to the structured MQS system (3.1).

3.1. Balanced truncation. We now apply a balanced truncation model reduction approach to the ODE system

$$\begin{aligned} E_1\dot{x}_1 &= A_1x_1 + B_1u, \\ y &= C_1x_1, \end{aligned} \tag{3.2}$$

with the system matrices

$$\begin{aligned} E_1 &= \begin{bmatrix} M_{11} + X_1 R^{-1} X_1^T & X_1 R^{-1} X_2^T Z \\ Z^T X_2 R^{-1} X_1^T & Z^T X_2 R^{-1} X_2^T Z \end{bmatrix}, \\ A_1 &= -\begin{bmatrix} K_{11} & K_{12} Z \\ Z^T K_{21} & Z^T K_{22} Z \end{bmatrix} + \begin{bmatrix} K_{12} \\ Z^T K_{22} \end{bmatrix} Y \left(Y^T K_{22} Y \right)^{-1} Y^T [K_{21},\, K_{22} Z], \\ B_1 &= \begin{bmatrix} X_1 \\ Z^T X_2 \end{bmatrix} R^{-1}, \\ C_1 &= -(X_2^T X_2)^{-1} X_2^T \left(I - K_{22} Y (Y^T K_{22} Y)^{-1} Y^T \right) [K_{21},\, K_{22} Z], \end{aligned} \tag{3.3}$$

which is equivalent the DAE system (3.1). This approach relies on the controllability and observability Gramians P and Q satisfying the generalized Lyapunov equations

$$A_1 P E_1^T + E_1 P A_1^T = -B_1 B_1^T, \tag{3.4}$$

$$A_1^T Q E_1 + E_1^T Q A_1 = -C_1^T C_1. \tag{3.5}$$

If the pencil $\lambda E_1 - A_1$ is stable, i.e., all its eigenvalues have negative real part, then these equations have unique symmetric, positive semidefinite solutions. The following lemma shows that the matrices E_1 and $-A_1$ in (3.3) are both symmetric and positive definite, and, hence, the pencil $\lambda E_1 - A_1$ is stable.

LEMMA 3.1. *If M_{11}, K and R are symmetric and positive definite, then E_1 and $-A_1$ in* (3.3) *are symmetric and positive definite.*

Proof. It follows from (2.14) that the matrix E_1 can be decomposed as

$$E_1 = T_1^T \begin{bmatrix} M_{11} & 0 \\ 0 & (X_2^T X_2)^{1/2} R^{-1} (X_2^T X_2)^{1/2} \end{bmatrix} T_1$$

with a nonsingular matrix

$$T_1 = \begin{bmatrix} I & 0 \\ (X_2^T X_2)^{-1/2} X_1^T & I \end{bmatrix}.$$

Since M_{11} and R are symmetric and positive definite, the matrix E_1 is symmetric and positive definite too.

Furthermore, observe that the matrix A_1 is the Schur complement of the symmetric, negative definite matrix

$$-\hat{T} \begin{bmatrix} K_{11} & K_{12} \\ K_{21} & K_{22} \end{bmatrix} \hat{T}^T = -\left[\begin{array}{cc|c} K_{11} & K_{12} Z & K_{12} Y \\ Z^T K_{21} & Z^T K_{22} Z & Z^T K_{22} Y \\ \hline Y^T K_{21} & Y^T K_{22} Z & Y^T K_{22} Y \end{array}\right] \tag{3.6}$$

with the orthogonal matrix

$$\hat{T} = \begin{bmatrix} I_{n_1} & 0 \\ 0 & Z^T \\ 0 & Y^T \end{bmatrix}. \tag{3.7}$$

Therefore, $-A_1$ is symmetric and positive definite [20]. ∎

Note that for 2D models, the matrix K is positive definite. In the 3D case, the gauge on the non-conducting subdomain guarantees the regularity of the pencil $\lambda \mathcal{E} - \mathcal{A}$, but it has zero eigenvalues. The stability of $\lambda \mathcal{E} - \mathcal{A}$ and also of $\lambda E_1 - A_1$

can be enforced either by full gauging or by projecting out the states corresponding to zero eigenvalues. Due to the divergence-free property of the winding function, one can show that such states are uncontrollable and unobservable and, hence, they can be removed from the system without changing the input-output relation [28].

Let $P = SS^T$ and $Q = LL^T$ be the Cholesky factorizations of the Gramians and let

$$L^T E_1 S = [\, U_1,\, U_0 \,] \begin{bmatrix} \Sigma_1 & \\ & \Sigma_0 \end{bmatrix} [\, V_1,\, V_0 \,]^T \tag{3.8}$$

be a singular value decomposition (SVD) of $L^T E_1 S$, where the matrices $[\, U_1,\, U_0 \,]$ and $[\, V_1,\, V_0 \,]$ are orthogonal, $\Sigma_1 = \mathrm{diag}(\sigma_1, \ldots, \sigma_r)$ and $\Sigma_0 = \mathrm{diag}(\sigma_{r+1}, \ldots, \sigma_n)$ with $\sigma_1 \geq \ldots \geq \sigma_r > \sigma_{r+1} \geq \ldots \geq \sigma_n$ called the Hankel singular values of (3.2). Then we compute the reduced-order model

$$\begin{aligned} \tilde{E}_1 \dot{\tilde{x}}_1 &= \tilde{A}_1 \tilde{x}_1 + \tilde{B}_1 u, \\ \tilde{y} &= \tilde{C}_1 \tilde{x}_1 \end{aligned} \tag{3.9}$$

by projection

$$\tilde{E}_1 = W^T E_1 V, \qquad \tilde{A}_1 = W^T A_1 V, \qquad \tilde{B}_1 = W^T B_1, \qquad \tilde{C}_1 = C_1 V$$

with the projection matrices

$$W = L U_1 \Sigma_1^{-1/2}, \qquad V = S V_1 \Sigma_1^{-1/2}. \tag{3.10}$$

An important property of balanced truncation is that the reduced-order model (3.9) satisfies the error bound

$$\| H - \tilde{H} \|_{\mathcal{H}_\infty} = \sup_{\omega \in \mathbb{R}} \| H(\mathrm{i}\omega) - \tilde{H}(\mathrm{i}\omega) \|_2 \leq 2(\sigma_{r+1} + \ldots + \sigma_n),$$

where

$$\begin{aligned} H(s) &= \mathcal{C}(s\,\mathcal{E} - \mathcal{A})^{-1} \mathcal{B} = C_1 (sE_1 - A_1)^{-1} B_1, \\ \tilde{H}(s) &= \tilde{C}_1 (s\tilde{E}_1 - \tilde{A}_1)^{-1} \tilde{B}_1 \end{aligned}$$

are the transfer functions of the original and reduced-order models, $\mathrm{i} = \sqrt{-1}$, and $\| \cdot \|_2$ denotes the spectral matrix norm, see [14]. Moreover, the balanced truncation method preserves stability in (3.9). It should, however, be noticed that the preservation of other properties, in particular, passivity cannot, in general, be guaranteed for this method. In the following, we will show that system (3.2) is actually passive and, fortunately, the balanced truncation method preserves passivity in the reduced-order model (3.9).

Definition 3.2. *System* (3.2) *is called* passive *if for all inputs* $u : [0, t_f) \to \mathbb{R}^m$ *and* $x_1(0) = 0$ *the corresponding output* $y : [0, t_f) \to \mathbb{R}^m$ *satisfies*

$$\int_0^{t_f} u(\tau)^T y(\tau) d\tau \geqslant 0.$$

It is well known [1] that system (3.2) is passive if and only if its transfer function $H(s) = C_1 (sE_1 - A_1)^{-1} B_1$ is *positive real*, i.e., $H(s)$ is analytic for all $s \in \mathbb{C}_+$, where $\mathbb{C}_+$ denotes the closed right half-plane, and $H(s) + H^T(\overline{s}) \geq 0$ for all $s \in \mathbb{C}_+$.

Sufficient conditions for (3.2) to be passive are the conditions

$$E_1 = E_1^T > 0, \qquad A_1 + A_1^T < 0, \qquad C_1 = B_1^T. \tag{3.11}$$

By Lemma 3.1 the first two conditions in (3.11) are satisfied. However, the third condition in (3.11) fails because, as it follows from (2.12c) and (2.15), we have

$$C_1 = -B_1^T E_1^{-1} A_1. \tag{3.12}$$

Nevertheless, passivity can be established for system (3.2).

THEOREM 3.3. *If M_{11}, K and R are symmetric, positive definite, then system* (3.2) *is passive.*

Proof. By Lemma 3.1 the matrices E_1 and $-A_1$ are symmetric, positive definite, and, hence, the transfer function $H(s)$ is analytic for all $s \in \mathbb{C}_+$. Taking into account (3.12), we have

$$\begin{aligned} H(s) + H^T(\overline{s}) &= C_1(sE_1 - A_1)^{-1}B_1 + B_1^T(\overline{s}E_1 - A_1)^{-1}C_1^T \\ &= F^*(s)\big(-E_1A_1^{-1}(\overline{s}E_1 - A_1) - (sE_1 - A_1)A_1^{-1}E_1\big)F(s) \\ &= 2F^*(s)\big(\mathrm{Re}(s)E_1(-A_1)^{-1}E_1 + E_1\big)F(s) \end{aligned}$$

with $F(s) = E_1^{-1}A_1(sE_1 - A_1)^{-1}B_1$. As $\mathrm{Re}(s)E_1(-A_1)^{-1}E_1 + E_1$ is positive definite for all $s \in \mathbb{C}_+$, the transfer function $H(s)$ is positive real, and, hence, system (3.2) is passive. □

The next theorem gives a useful relationship between the Gramians P and Q of system (3.2), (3.3).

THEOREM 3.4. *Let P and Q be the solutions of the Lyapunov equations* (3.4) *and* (3.5)*, respectively. If M_{11}, K, and R are symmetric, positive definite, then*

$$E_1QE_1 = A_1PA_1. \tag{3.13}$$

Proof. The left and right multiplication of the Lyapunov equations (3.4) and (3.5) by E_1^{-1} and A_1^{-1}, respectively, yields

$$\begin{aligned} E_1^{-1}A_1P + PA_1E_1^{-1} &= -E_1^{-1}B_1B_1^TE_1^{-1}, \\ QE_1A_1^{-1} + A_1^{-1}E_1Q &= -E_1^{-1}B_1B_1^TE_1^{-1}. \end{aligned}$$

Introducing $P_s = A_1PA_1$ and $Q_s = E_1QE_1$, these equations can be written as

$$\begin{aligned} E_1^{-1}P_sA_1^{-1} + A_1^{-1}P_sE_1^{-1} &= -E_1^{-1}B_1B_1^TE_1^{-1}, \\ E_1^{-1}Q_sA_1^{-1} + A_1^{-1}Q_sE_1^{-1} &= -E_1^{-1}B_1B_1^TE_1^{-1}. \end{aligned}$$

Since P_s and Q_s solve the same Lyapunov equation which is uniquely solvable, we have $P_s = Q_s$, and, hence, (3.13) holds. □

The relation (3.13) implies that once we compute the Cholesky factor S of the controllability Gramian $P = SS^T$, the Cholesky factor L of the observability Gramian can be determined from $Q = E_1^{-1}A_1SS^TA_1E_1^{-1} = LL^T$ as $L = -E_1^{-1}A_1S$. This implies that the matrix $L^TE_1S = -S^TA_1S$ is symmetric, positive semidefinite. Therefore, we compute the eigenvalue decomposition (EVD)

$$-S^TA_1S = [\,U_1,\ U_0\,]\begin{bmatrix}\Lambda_1 & \\ & \Lambda_0\end{bmatrix}[\,U_1,\ U_0\,]^T,$$

instead of the more expensive SVD (3.8). Then the projection matrices in (3.10) take the form

$$V = SU_1\Lambda_1^{-1/2}, \qquad W = -E_1^{-1}A_1SU_1\Lambda_1^{-1/2} = -E_1^{-1}A_1V.$$

Applying the Petrov-Galerkin projection to (3.2), we obtain the reduced-order model (3.9) with

$$\begin{aligned}
\tilde{E}_1 &= W^TE_1V = -V^TA_1E_1^{-1}E_1V = I,\\
\tilde{A}_1 &= W^TA_1V = -\Lambda_1^{-1/2}U_1^TS^TA_1E_1^{-1}A_1SU_1\Lambda_1^{-1/2},\\
\tilde{B}_1 &= W^TB_1 = -\Lambda_1^{-1/2}U_1^TS^TA_1E_1^{-1}B_1,\\
\tilde{C}_1 &= C_1V = -B_1^TE_1^{-1}A_1SU_1\Lambda_1^{-1/2}.
\end{aligned} \tag{3.14}$$

We note that $\tilde{E}_1 = \tilde{E}_1^T > 0$, $\tilde{A}_1 = \tilde{A}_1^T < 0$ and $\tilde{C}_1 = \tilde{B}_1^T$, and, hence, system (3.9) is passive. Thus, for system (3.2) with symmetric, positive definite matrices E_1, $-A_1$ and the input and output matrices related by (3.12), the balanced truncation method preserves passivity. It involves the numerical solution of one Lyapunov equation only and the computation of the eigenvalue decomposition.

3.2. Numerical aspects. For solving the generalized Lyapunov equation (3.4), we employ the low-rank alternating direction implicit (LR-ADI) method proposed first in [24, 32] and then significantly improved in [4, 5]. The LR-ADI iteration for the Lyapunov equation (3.4) has the form

$$\begin{aligned}
F_k &= (\tau_kE_1 + A_1)^{-1}Y_{k-1},\\
Y_k &= Y_{k-1} - 2\mathrm{Re}(\tau_k)E_1\,F_k,\\
Z_k &= [Z_{k-1},\ \sqrt{-2\mathrm{Re}(\tau_k)}\,F_k\,]
\end{aligned} \tag{3.15}$$

with the initial matrices $Y_0 = B$, $Z_0 = [\ ]$ and shift parameters $\tau_k \in \mathbb{C}_-$. Then the solution of (3.4) is approximated by $P \approx Z_kZ_k^T$ and $Z_k \in \mathbb{R}^{n,mk}$ is said to be a low-rank Cholesky factor of P. The LR-ADI iteration (3.15) can be stopped once the residual

$$A_1Z_kZ_k^TE_1^T + E_1Z_kZ_k^TA_1^T + B_1B_1^T = Y_kY_k^T$$

satisfies the condition $\|Y_kY_k^T\|_F = \|Y_k^TY_k\|_F \le tol\|B_1^TB_1\|_F$ with a given tolerance tol. Here, $\|\cdot\|_F$ denotes the Frobenius matrix norm.

The main computational effort in the LR-ADI iteration (3.15) is the numerical solution of linear systems with the matrices $\tau E_1 + A_1$. Note that although $\mathcal{E}$ and $\mathcal{A}$ in (3.1) are sparse, the matrices E_1 and A_1 in (3.3) are, in general, dense. This prohibits the use of iterative sparse linear system solvers. Therefore, E_1 and A_1 will never be constructed explicitly, but instead their block structure should be exploited to compute $(\tau E_1 + A_1)^{-1}v$ for a vector v. The following lemma shows that this product can be determined by solving a sparse linear system.

LEMMA 3.5. *Let E_1 and A_1 be as in (3.3), $Z = X_2(X_2^TX_2)^{-1/2}$, $\tau \in \mathbb{C}$ and $[v_1^T, v_2^T]^T \in \mathbb{R}^{n_1+m}$. Then the vector*

$$z = (\tau E_1 + A_1)^{-1}\begin{bmatrix} v_1 \\ v_2 \end{bmatrix}$$

can be determined as $z = [z_1^T, (Z^Tz_2)^T]^T$, where z_1 and z_2 satisfy the sparse linear system

$$(\tau\mathcal{E} + \mathcal{A})\begin{bmatrix} z_1 \\ z_2 \\ z_3 \end{bmatrix} = \begin{bmatrix} v_1 \\ Zv_2 \\ 0 \end{bmatrix} \tag{3.16}$$

with $\mathcal{E}$ and $\mathcal{A}$ given in (2.3).

Proof. Multiplying system (3.16) from the left with the orthogonal matrix T as in (2.9) and taking into account that $Y^TX_2 = 0$ and $YY^T + ZZ^T = I$, we have

$$\begin{aligned}
(\tau M_{11} - K_{11})z_1 - K_{12}Z(Z^Tz_2) - K_{12}Y(Y^Tz_2) + X_1z_3 &= v_1,\\
-Z^TK_{21}z_1 - Z^TK_{22}Z(Z^Tz_2) - Z^TK_{22}Y(Y^Tz_2) + Z^TX_2z_3 &= v_2,\\
-Y^TK_{21}z_1 - Y^TK_{22}Z(Z^Tz_2) - Y^TK_{22}Y(Y^Tz_2) &= 0,\\
\tau X_1^Tz_1 + \tau X_2^TZ(Z^Tz_2) + -Rz_3 &= 0.
\end{aligned}$$

Solving the third and fourth equations for

$$\begin{aligned}
Y^Tz_2 &= -(Y^TK_{22}Y)^{-1}\left[\, Y^TK_{21},\ Y^TK_{22}Z \,\right]\begin{bmatrix} z_1 \\ Z^Tz_2 \end{bmatrix},\\
z_3 &= \tau R^{-1}\left[\, X_1^T,\ X_2^TZ \,\right]\begin{bmatrix} z_1 \\ Z^Tz_2 \end{bmatrix}
\end{aligned}$$

and substituting these vectors into the first and second equations, we obtain

$$(\tau E_1 + A_1)\begin{bmatrix} z_1 \\ Z^Tz_2 \end{bmatrix} = \begin{bmatrix} v_1 \\ v_2 \end{bmatrix}.$$

The nonsingularity of $\tau E_1 + A_1$ implies that $z = [z_1^T, (Z^Tz_2)^T]^T$. ∎

The convergence rate of the LR-ADI iteration (3.15) strongly depends on the choice of the shift parameters. They can be determined, for example, from largest and smallest Ritz values of the pencil $\lambda E_1 - A_1$ computed by an Arnoldi procedure applied to $E_1^{-1}A_1$ and $A_1^{-1}E_1$, respectively, see [32]. Other approaches for computing shift parameters can be found in [6]. Again, we can use the special structure of E_1 and A_1 in (3.3) to construct the vectors $E_1^{-1}A_1v$ and $A_1^{-1}E_1v$ required in the Arnoldi procedure. First, we show that the computation of Y needed in A_1 can completely be avoided.

LEMMA 3.6. *Let $X_2 \in \mathbb{R}^{n_2,m}$ be of full column rank, $K_{22} \in \mathbb{R}^{n_2,n_2}$ and $w \in \mathbb{R}^{n_2}$. Assume that the columns of $Y \in \mathbb{R}^{n_2,n_2-m}$ form a basis of* $\ker(X_2^T)$. *If $[z_1^T, z_2^T]^T$ solves the linear system*

$$\begin{bmatrix} K_{22} & X_2 \\ X_2^T & 0 \end{bmatrix}\begin{bmatrix} z_1 \\ z_2 \end{bmatrix} = \begin{bmatrix} w \\ 0 \end{bmatrix}, \tag{3.17}$$

then $z_1 = Y(Y^TK_{22}Y)^{-1}Y^Tw$.

Proof. The second equation in (3.17) implies that $z_1 \in \ker(X_2^T) = \mathrm{im}(Y)$. Hence, there exists $g \in \mathbb{R}^{n_2-m}$ such that $z_1 = Yg$. Substituting this vector into the first equation in (3.17) and multiplying it from the left with the matrix Y^T, we obtain $Y^TK_{22}Yg = Y^Tw$. Then $z_1 = Yg = Y(Y^TK_{22}Y)^{-1}Y^Tw$. ∎

Taking into account the structure of A_1 and E_1^{-1} in (3.3) and (2.13), respectively, and Lemma 3.6, the vector $z = E_1^{-1}A_1v$ can be computed by Algorithm 1.

Next, we consider the computation of the vector $z = A_1^{-1}E_1v$. Since A_1 is the Schur complement of the matrix in (3.6), the vector $z = [z_1^T, z_2^T]^T = A_1^{-1}E_1v$ satisfies the linear system

$$-\hat{T}\begin{bmatrix} K_{11} & K_{12} \\ K_{21} & K_{22} \end{bmatrix}\hat{T}^T\begin{bmatrix} z_1 \\ z_2 \\ z_3 \end{bmatrix} = \begin{bmatrix} E_1v \\ 0 \end{bmatrix}, \tag{3.18}$$

Algorithm 1 Computation of $E_1^{-1}A_1v$.

Input: M_{11}, $K_{11} \in \mathbb{R}^{n_1,n_1}$, $K_{12} \in \mathbb{R}^{n_1,n_2}$, $K_{21} \in \mathbb{R}^{n_2,n_1}$, $K_{22} \in \mathbb{R}^{n_2,n_2}$, $X_1 \in \mathbb{R}^{n_1,m}$, $X_2 \in \mathbb{R}^{n_2,m}$, $v = [v_1^T, v_2^T]^T \in \mathbb{R}^{n_1+m}$

Output: $z = E_1^{-1}A_1v$ with E_1 and A_1 as in (2.12a) and (2.12b), respectively.

1: Compute $\hat{v}_2 = X_2(X_2^TX_2)^{-1/2}v_2$.

2: Solve the linear system

$$\begin{bmatrix} K_{22} & X_2 \\ X_2^T & 0 \end{bmatrix} \begin{bmatrix} z_1 \\ z_2 \end{bmatrix} = \begin{bmatrix} K_{21}v_1 + K_{22}\hat{v}_2 \\ 0 \end{bmatrix}.$$

3: Compute

$$\begin{bmatrix} \hat{z}_1 \\ \hat{z}_2 \end{bmatrix} = -\begin{bmatrix} K_{11} & K_{12} \\ K_{21} & K_{22} \end{bmatrix} \begin{bmatrix} v_1 \\ \hat{v}_2 \end{bmatrix} + \begin{bmatrix} K_{12} \\ K_{22} \end{bmatrix} z_1.$$

4: Compute $w_2 = (X_2^TX_2)^{-1}X_2^T\hat{z}_2$.

5: Solve the linear system $M_{11}w_1 = \hat{z}_1 - X_1w_2$.

6: Compute

$$z = \begin{bmatrix} w_1 \\ -(X_2^TX_2)^{-1/2}(X_1^Tw_1 - Rw_2) \end{bmatrix}.$$

with orthogonal $\hat{T}$ given in (3.7). For $v = [v_1^T, v_2^T]^T$, we introduce

$$f = \hat{T}^T \begin{bmatrix} E_1v \\ 0 \end{bmatrix} = \begin{bmatrix} I & 0 \\ 0 & Z \end{bmatrix} E_1v = \begin{bmatrix} M_{11}v_1 + X_1R^{-1}(X_1^Tv_1 + (X_2^TX_2)^{1/2}v_2) \\ X_2R^{-1}(X_1^Tv_1 + (X_2^TX_2)^{1/2}v_2) \end{bmatrix}$$

and set

$$\begin{bmatrix} \hat{z}_1 \\ \hat{z}_2 \end{bmatrix} = \hat{T}^T \begin{bmatrix} z_1 \\ z_2 \\ z_3 \end{bmatrix}. \tag{3.19}$$

Then the linear system (3.18) can be written as

$$-\begin{bmatrix} K_{11} & K_{12} \\ K_{21} & K_{22} \end{bmatrix} \begin{bmatrix} \hat{z}_1 \\ \hat{z}_2 \end{bmatrix} = f.$$

Using the orthogonality of $[Z, Y]$, we obtain from (3.19) that

$$\begin{bmatrix} z_1 \\ z_2 \end{bmatrix} = \begin{bmatrix} \hat{z}_1 \\ Z^T\hat{z}_2 \end{bmatrix}.$$

The computation of $z = A_1^{-1}E_1v$ is summarized in Algorithm 2.

Finally, we present in Algorithm 3 the computation of the reduced-order matrices $\tilde{A}_1$, $\tilde{B}_1$ and $\tilde{C}_1$ as in (3.14). The first three steps there are similar to those in Algorithm 1. Computing $\hat{Z}_1$ and $\hat{Z}_2$ in Step 3 of Algorithm 3, we have

$$A_1V = \begin{bmatrix} \hat{Z}_1 \\ (X_2^TX_2)^{-1/2}X_2^T\hat{Z}_2 \end{bmatrix}, \quad W = -E_1^{-1}A_1V = \begin{bmatrix} -W_1 \\ (X_2^TX_2)^{-1/2}(X_1^TW_1 - RW_2) \end{bmatrix},$$

Algorithm 2 Computation of $A_1^{-1}E_1v$.

Input: M_{11}, $K_{11} \in \mathbb{R}^{n_1,n_1}$, $K_{12} \in \mathbb{R}^{n_1,n_2}$, $K_{21} \in \mathbb{R}^{n_2,n_1}$, $K_{22} \in \mathbb{R}^{n_2,n_2}$, $X_1 \in \mathbb{R}^{n_1,m}$, $X_2 \in \mathbb{R}^{n_2,m}$, $v = [v_1^T, v_2^T]^T \in \mathbb{R}^{n_1+m}$.

Output: $z = A_1^{-1}E_1v$ with E_1 and A_1 as in (2.12a) and (2.12b), respectively.

1: Compute $w = R^{-1}(X_1^Tv_1 + (X_2^TX_2)^{1/2}v_2)$.

2: Solve the linear system

$$-\begin{bmatrix} K_{11} & K_{12} \\ K_{21} & K_{22} \end{bmatrix}\begin{bmatrix} \hat{z}_1 \\ \hat{z}_2 \end{bmatrix} = \begin{bmatrix} M_{11}v_1 + X_1w \\ X_2w \end{bmatrix}.$$

3: Compute

$$z = \begin{bmatrix} \hat{z}_1 \\ (X_2^TX_2)^{-1/2}X_2^T\hat{z}_2 \end{bmatrix}.$$

Algorithm 3 Computation of the reduced-order matrices.

Input: M_{11}, $K_{11} \in \mathbb{R}^{n_1,n_1}$, $K_{12} \in \mathbb{R}^{n_1,n_2}$, $K_{21} \in \mathbb{R}^{n_2,n_1}$, $K_{22} \in \mathbb{R}^{n_2,n_2}$, $X_1 \in \mathbb{R}^{n_1,m}$, $X_2 \in \mathbb{R}^{n_2,m}$, $R \in \mathbb{R}^{m,m}$, and $V = [V_1^T, V_2^T]^T \in \mathbb{R}^{n_1+m,r}$.

Output: $\tilde{A}_1$, $\tilde{B}_1$ and $\tilde{C}_1$ as in (3.14).

1: Compute $\hat{V}_2 = X_2(X_2^TX_2)^{-1/2}V_2$.

2: Solve the linear system

$$\begin{bmatrix} K_{22} & X_2 \\ X_2^T & 0 \end{bmatrix}\begin{bmatrix} Z_1 \\ Z_2 \end{bmatrix} = \begin{bmatrix} K_{21}V_1 + K_{22}\hat{V}_2 \\ 0 \end{bmatrix}.$$

3: Compute

$$\begin{bmatrix} \hat{Z}_1 \\ \hat{Z}_2 \end{bmatrix} = -\begin{bmatrix} K_{11} & K_{12} \\ K_{21} & K_{22} \end{bmatrix}\begin{bmatrix} V_1 \\ \hat{V}_2 \end{bmatrix} + \begin{bmatrix} K_{12} \\ K_{22} \end{bmatrix} Z_1.$$

4: Compute $\tilde{C}_1 = -(X_2^TX_2)^{-1}X_2^T\hat{Z}_2$ and $\tilde{B}_1 = \tilde{C}_1^T$.

5: Compute $\tilde{A}_1 = -(\hat{Z}_1 + X_1\tilde{C}_1)^TM_{11}^{-1}(\hat{Z}_1 + X_1\tilde{C}_1) - \tilde{C}_1^TR\tilde{C}_1$.

where $W_2 = (X_2^TX_2)^{-1}X_2^T\hat{Z}_2$ and W_1 solves $M_{11}W_1 = \hat{Z}_1 - X_1W_2$ (compare Steps 4-6 in Algorithm 1). Then exploiting the block structure of A_1 and B_1 in (3.3), we obtain

$$\begin{aligned} \tilde{C}_1 &= B_1^TW = R^{-1}(-X_1^TW_1 + X_1^TW_1 - RW_2) = -W_2 = \tilde{B}_1^T, \\ \tilde{A}_1 &= W^TA_1V = -W_1^T\hat{Z}_1 + (W_1^TX_1 - W_2^TR)(X_2^TX_2)^{-1}X_2^T\hat{Z}_2 \\ &= -(\hat{Z}_1 - X_1W_2)^TM_{11}^{-1}(\hat{Z}_1 - X_1W_2) - W_2^TRW_2. \end{aligned}$$

This justifies the last two steps in Algorithm 3.

4. Model reduction of nonlinear MQS systems. In this section, we consider model reduction of the nonlinear MQS system (2.2) using the proper orthogonal decomposition (POD) approach, e.g., [44], combined with the discrete empirical interpolation method (DEIM) [11].

4.1. Proper orthogonal decomposition. The POD method applied to the nonlinear DAE (2.2) consists in constructing a snapshot matrix $\mathcal{X} = [x(t_1), \ldots, x(t_q)]$

and computing the SVD

$$\mathcal{X} = [\, U,\, U_0 \,] \begin{bmatrix} \Sigma & \\ & \Sigma_0 \end{bmatrix} [\, V,\, V_0 \,]^T$$

with $\Sigma = \mathrm{diag}(\sigma_1, \ldots, \sigma_r)$, $\Sigma_0 = \mathrm{diag}(\sigma_{r+1}, \ldots, \sigma_q)$ and $\sigma_1 \geq \ldots \geq \sigma_r > \sigma_{r+1} \geq \ldots \geq \sigma_q$. Then a reduced-order model can be determined by projecting

$$\begin{aligned} \tilde{\mathcal{E}}\, \dot{\tilde{x}} &= \tilde{\mathcal{A}}(\tilde{x})\, \tilde{x} + \tilde{\mathcal{B}}\, u, \\ \tilde{y} &= \tilde{\mathcal{C}}\, \tilde{x}, \end{aligned} \tag{4.1}$$

where $\tilde{x} \in \mathbb{R}^r$, $\tilde{\mathcal{E}} = U^T \mathcal{E} U$, $\tilde{\mathcal{A}}(\tilde{x}) = U^T \mathcal{A}(U\tilde{x})U$, $\tilde{\mathcal{B}} = U^T \mathcal{B}$, and $\tilde{\mathcal{C}} = \mathcal{C}U$. The columns of U are referred to as the POD basis of $\mathcal{X}$. This naive model reduction approach has several disadvantages. First note that the differential and algebraic components of the state vector x are mixed in the reduced-order model (4.1). Secondly, it is well known that the reduction of the algebraic components and the algebraic constraints in DAEs may lead to inaccurate and physically meaningless results, see [40].

To overcome these difficulties, we propose, as in the linear case, to transform the DAE (2.2) to the ODE form (2.8) with $x_1 = \left[\, a_1^T,\, a_{21}^T \,\right]^T$ and reduce the vector a_1 only, remaining a_{21} unchanged since it usually has only a few components. This can be done by partitioning the transformed snapshot matrix

$$T\mathcal{X} = \begin{bmatrix} \mathcal{X}_{a_1} \\ \mathcal{X}_{a_{21}} \\ \mathcal{X}_{a_{22}} \\ \mathcal{X}_{\iota} \end{bmatrix}$$

in blocks according to T in (2.9) and computing the SVD

$$\mathcal{X}_{a_1} = \left[\, U_{a_1},\, \hat{U}_{a_1} \,\right] \begin{bmatrix} \Sigma_{a_1} & \\ & \hat{\Sigma}_{a_1} \end{bmatrix} \left[\, V_{a_1},\, \hat{V}_{a_1} \,\right]^T, \tag{4.2}$$

where $\Sigma_{a_1} \in \mathbb{R}^{r_1, r_1}$ contains the dominant singular values of $\mathcal{X}_{a_1}$. Then the reduced-order model is obtained by projecting

$$\begin{aligned} \tilde{E}_1 \dot{\tilde{x}}_1 &= \tilde{A}_1(\tilde{x}_1)\tilde{x}_1 + \tilde{B}_1 u, \\ \tilde{y} &= \tilde{C}_1 \tilde{x}_1, \end{aligned} \tag{4.3}$$

where $\tilde{x}_1 = [\tilde{a}_1^T, a_{21}^T]^T$, $\tilde{E}_1 = U^T E_1 U$, $\tilde{A}_1(\tilde{x}_1) = U^T A_1(U\tilde{x}_1)U$, $\tilde{B}_1 = U^T B_1$, and $\tilde{C}_1 = C_1 U$ with the projection matrix

$$U = \begin{bmatrix} U_{a_1} & \\ & I_m \end{bmatrix}. \tag{4.4}$$

Note that the snapshot matrix $\mathcal{X}_{a_1}$ is determined by solving the DAE (2.2) and, similarly to the linear case, see Algorithm 3, the reduced-order matrices in (4.3) can be computed from (2.2) without forming the system matrices (2.12), (2.15). The proposed model reduction approach for the DAE (2.2) is referred to as *first transform* (to the ODE form), *then reduce*. On the other hand, we can *first reduce* the DAE (2.2) using the projection matrix

$$\begin{bmatrix} U_{a_1} & & \\ & Z^T & \\ & Y^T & \\ & & I_m \end{bmatrix}$$

and *then transform* the resulting system to the ODE form by eliminating the algebraic components. It turns out that for the DAE (2.2), these two approaches are equivalent in the sense that they provide the same reduced-order models. This does not necessarily hold for general DAEs.

4.2. Discrete empirical interpolation. In order to speed up the simulation of the reduced-order model (4.3), we employ further the DEIM [11] for efficient evaluation of the nonlinearity

$$\tilde{A}_1(\tilde{x}_1)\tilde{x}_1 = U^T A_1(U\tilde{x}_1)U\tilde{x}_1. \tag{4.5}$$

Taking into account the structure of the matrix $A_1(x_1)$ in (2.12b), the nonlinearity $A_1(x_1)x_1$ of system (2.8) can be written as

$$A_1(x_1)x_1 = A_l x_1 + \begin{bmatrix} f(a_1) \\ 0 \end{bmatrix}$$

with a constant matrix

$$A_l = -\begin{bmatrix} K_{11,l} & K_{12}Z \\ Z^T K_{21} & Z^T K_{22} Z \end{bmatrix} + \begin{bmatrix} K_{12} \\ Z^T K_{22} \end{bmatrix} Y \left(Y^T K_{22} Y\right)^{-1} Y^T [K_{21},\, K_{22}Z]$$

and a nonlinear function $f(a_1) = K_{11,n}(a_1)a_1$. Collecting the snapshots

$$\mathcal{X}_f = [f(a_1(t_1)), \ldots, f(a_1(t_q))], \tag{4.6}$$

we compute the SVD

$$\mathcal{X}_f = \begin{bmatrix} U_f,\, \hat{U}_f \end{bmatrix} \begin{bmatrix} \Sigma_f & \\ & \hat{\Sigma}_f \end{bmatrix} \begin{bmatrix} V_f,\, \hat{V}_f \end{bmatrix}^T, \tag{4.7}$$

where $\Sigma_f \in \mathbb{R}^{\ell,\ell}$ contains the dominant singular values of $\mathcal{X}_f$. Then the nonlinear function (4.5) can be approximated by

$$\tilde{A}_1(\tilde{x}_1)\tilde{x}_1 = U^T A_1(U\tilde{x}_1)U\tilde{x}_1 \approx U^T A_l U\tilde{x}_1 + \begin{bmatrix} \tilde{f}(\tilde{a}_1) \\ 0 \end{bmatrix} \tag{4.8}$$

with

$$\tilde{f}(\tilde{a}_1) = U_{a_1}^T U_f (S_{\mathcal{K}}^T U_f)^{-1} S_{\mathcal{K}}^T f(U_{a_1}\tilde{a}_1), \tag{4.9}$$

where $\mathcal{K} = \{k_1, \ldots, k_\ell\}$ is a DEIM index set determined from U_f using the Greedy algorithm as described in [11] and $S_{\mathcal{K}} = [\, e_{k_1}, \ldots, e_{k_\ell}] \in \mathbb{R}^{n_1,\ell}$ is the selector matrix associated with $\mathcal{K}$. Here, e_j denotes the j-th column of the $n_1 \times n_1$ identity matrix. Note that the time-independent matrices $U^T A_l U$ and $U_{a_1}^T U_f (S_{\mathcal{K}}^T U_f)^{-1}$ can be precomputed and stored in the offline stage. Then in the online stage, we evaluate only ℓ components of the function $f(U_{a_1}\tilde{a}_1)$ given by

$$f_k(U_{a_1}\tilde{a}_1) = \int_{\Omega_1} \nu_1(\|\nabla \times \sum_{i=1}^{n_1} \tilde{\alpha}_i \varphi_i\|^2)(\nabla \times \sum_{i=1}^{n_1} \tilde{\alpha}_i \varphi_i) \cdot (\nabla \times \varphi_k)\, d\xi, \quad k \in \mathcal{K}, \tag{4.10}$$

where $U_{a_1}\tilde{a}_1 = [\tilde{\alpha}_1, \ldots \tilde{\alpha}_{n_1}]^T$. A further reduction in computational complexity can be achieved by taking into account that the integrals in (4.10) have to be computed

on $\mathrm{supp}(\varphi_k)$, $k \in \mathcal{K}$, which are small subdomains of Ω. As a consequence, only a few components of the vector $U_{a_1}\tilde{a}_1$ are required to evaluate $S_{\mathcal{K}}^T f(U_{a_1}\tilde{a}_1)$. To find such components, we introduce an index set

$$\mathcal{K}_{ext,k} = \Big\{\, i \in \{1,\ldots,n_1\} \;\; : \;\; \mathring{\mathrm{supp}}(\varphi_i) \cap \mathring{\mathrm{supp}}(\varphi_k) \neq \emptyset \,\Big\}, \tag{4.11}$$

where $\mathring{\mathrm{supp}}(\varphi_k)$ denotes the interior of $\mathrm{supp}(\varphi_k)$. With this extended index set we have

$$\sum_{i=1}^{n_1} \tilde{\alpha}_i \varphi_i = \sum_{i \in \mathcal{K}_{ext,k}} \tilde{\alpha}_i \varphi_i \quad \text{on } \mathrm{supp}(\varphi_k).$$

Then the integral (4.10) can be simplified to

$$f_k(U_{a_1}\tilde{a}_1) = \int\limits_{\mathrm{supp}(\varphi_k)} \nu_1(\|\nabla \times \sum_{i \in \mathcal{K}_{ext,k}} \tilde{\alpha}_i \varphi_i\|^2)(\nabla \times \sum_{i \in \mathcal{K}_{ext,k}} \tilde{\alpha}_i \varphi_i) \cdot (\nabla \times \varphi_k)\, d\xi, \;\; k \in \mathcal{K}.$$

One can see that to evaluate the function $S_{\mathcal{K}}^T f(U_{a_1}\tilde{a}_1)$, we do not need all components of $U_{a_1}\tilde{a}_1 \in \mathbb{R}^{n_1}$, but rather only those from the index set

$$\mathcal{K}_{ext} = \bigcup_{k \in \mathcal{K}} \mathcal{K}_{ext,k}.$$

The number of elements of $\mathcal{K}_{ext}$, denoted by $|\mathcal{K}_{ext}|$, is much smaller than n_1. In this case, we can shortly write

$$S_{\mathcal{K}}^T f(U_{a_1}\tilde{a}_1) = \hat{f}(S_{\mathcal{K}_{ext}}^T U_{a_1}\tilde{a}_1), \tag{4.12}$$

where $S_{\mathcal{K}_{ext}}$ is the selector matrix associated with $\mathcal{K}_{ext}$ and $\hat{f} : \mathbb{R}^{|\mathcal{K}_{ext}|} \to \mathbb{R}^{\ell}$ coincides with $S_{\mathcal{K}}^T f$ but unlike $S_{\mathcal{K}}^T f$ depends on the selected components of $U_{a_1}\tilde{a}_1$ only. Thus, we can calculate the DEIM approximation $\tilde{f}(\tilde{a}_1) = U_{a_1}^T U_f (S_{\mathcal{K}}^T U_f)^{-1} \hat{f}(S_{\mathcal{K}_{ext}}^T U_{a_1}\tilde{a}_1)$ independently from the original size n_1.

We consider now the reduced-order model (4.3) with $\tilde{A}_1(\tilde{x}_1)\tilde{x}_1$ replaced by the POD-DEIM approximation as in (4.8), (4.9). Integrating this system in time using a one-step or multistep method [15], we face with the problem of solving a sequence of systems of nonlinear equations. For this purpose, we employ the Newton iteration which requires the computation of the Jacobi matrix $J_{\tilde{f}}(\tilde{a}_1)$ of the nonlinear function $\tilde{f}$ at $\tilde{a}_1$. This matrix has the form

$$J_{\tilde{f}}(\tilde{a}_1) = U_{a_1}^T U_f (S_{\mathcal{K}}^T U_f)^{-1} S_{\mathcal{K}}^T J_f(U_{a_1}\tilde{a}_1)\, U_{a_1},$$

where $J_f(U_{a_1}\tilde{a}_1)$ is the Jacobi matrix of f at $U_{a_1}\tilde{a}_1$. In the case of the sparse matrix $S_{\mathcal{K}}^T J_f(U_{a_1}\tilde{a}_1)$, we introduce an index set

$$\mathcal{J} = \{\; (i,j) \quad : \quad \big(S_{\mathcal{K}}^T J_f(U_{a_1}\tilde{a}_1)\big)_{i,j} \neq 0 \;\}$$

of non-zero entries of this matrix. Let $\Theta_{(i,j)} \in \mathbb{R}^{\ell,n_1}$ have all zero entries except for the (i,j)-th entry being 1. Then the Jacobi matrix $J_{\tilde{f}}(\tilde{a}_1)$ admits an affine representation

$$J_{\tilde{f}}(\tilde{a}_1) = \sum_{(i,j) \in \mathcal{J}} U_{a_1}^T U_f (S_{\mathcal{K}}^T U_f)^{-1} \Theta_{(i,j)} U_{a_1} \big(S_{\mathcal{K}}^T J_f(U_{a_1}\tilde{a}_1)\big)_{i,j},$$

where the time-independent matrices $U_{a_1}^T U_f (S_\mathcal{K}^T U_f)^{-1} \Theta_{(i,j)} U_{a_1} \in \mathbb{R}^{r_1, r_1}$ can be pre-computed and stored in the offline phase, and only a small number of the time-dependent functions $\left(S_\mathcal{K}^T J_f(U_{a_1}\tilde{a}_1)\right)_{i,j}$, $(i,j) \in \mathcal{J}$, have to be evaluated in the online phase.

4.3. Matrix discrete empirical interpolation. An alternative approach for the efficient evaluation of the Jacobi matrix $J_{\tilde{f}}(\tilde{a}_1)$ in the online stage is based on a matrix discrete empirical interpolation method (MDEIM) [46]. Our goal is to find an approximation

$$S_\mathcal{K}^T J_f(U_{a_1}\tilde{a}_1) \approx \sum_{l=1}^{p} V_l \, g_l(U_{a_1}\tilde{a}_1) \tag{4.13}$$

with $V_l \in \mathbb{R}^{\ell, n_1}$, $g_l(U_{a_1}\tilde{a}_1) \in \mathbb{R}$ and $p \ll n_1$. Then the reduced Jacobi matrix $J_{\tilde{f}}(\tilde{a}_1)$ is approximated by

$$J_{\tilde{f}}(\tilde{a}_1) \approx \sum_{l=1}^{p} U_{a_1}^T U_f (S_\mathcal{K}^T U_f)^{-1} V_l \, U_{a_1} g_l(U_{a_1}\tilde{a}_1),$$

where the time-independent reduced matrices $U_{a_1}^T U_f (S_\mathcal{K}^T U_f)^{-1} V_l U_{a_1}$ can be pre-computed and stored in the offline stage, and only the evaluation of the p scalar functions $g_l(U_{a_1}\tilde{a}_1)$ is required in the online stage.

The MDEIM approximation of $S_\mathcal{K}^T J_f(U_{a_1}\tilde{a}_1)$ can be determined by DEIM using the vectorization operator [46]. Here, we use an efficient formulation of MDEIM proposed first in [42]. To find the MDEIM approximation (4.13), we collect the snapshots $J_1 = S_\mathcal{K}^T J_f(a_1(t_1)), \ldots, J_q = S_\mathcal{K}^T J_f(a_1(t_q))$ and construct a matrix

$$\mathcal{X}_J = \begin{bmatrix} \langle J_1, J_1 \rangle_F & \cdots & \langle J_1, J_q \rangle_F \\ \vdots & \ddots & \vdots \\ \langle J_q, J_1 \rangle_F & \cdots & \langle J_q, J_q \rangle_F \end{bmatrix}, \tag{4.14}$$

where $\langle J_i, J_j \rangle_F = \mathrm{trace}(J_j^T J_i)$ denotes the Frobenius inner product of the matrices J_i and J_j. The matrix $\mathcal{X}_J$ is symmetric and positive semidefinite. Computing the EVD

$$\mathcal{X}_J = \begin{bmatrix} W_J, \, \hat{W}_J \end{bmatrix} \begin{bmatrix} \Lambda_J & \\ & \hat{\Lambda}_J \end{bmatrix} \begin{bmatrix} W_J, \, \hat{W}_J \end{bmatrix}^T, \tag{4.15}$$

where $\Lambda_J \in \mathbb{R}^{p,p}$ contains p dominant eigenvalues of $\mathcal{X}_J$, the POD basis matrices V_l can then be determined as

$$V_l = \sum_{k=1}^{q} J_k w_{kl}, \qquad l = 1, \ldots, p, \tag{4.16}$$

where w_{kl} are the entries of the matrix $W_J \Lambda_J^{-1/2} \in \mathbb{R}^{q,p}$. Note that the basis matrices V_l in (4.16) have the same sparsity pattern as $S_\mathcal{K}^T J_f(U_{a_1}\tilde{a}_1)$ and, as the following lemma shows, they are orthogonal with respect to the Frobenius inner product.

LEMMA 4.1. *The matrices V_l in (4.16) fulfil $\langle V_l, V_j \rangle_F = \delta_{lj}$, where δ_{lj} is the Kronecker delta.*

Proof. It follows from the EVD (4.15) and (4.16) that

$$\begin{aligned}\langle V_l, V_j\rangle_F &= \operatorname{trace}\Big(\Big(\sum_{k=1}^{q} J_k w_{kl}\Big)^T \Big(\sum_{i=1}^{q} J_i w_{ij}\Big)\Big) = \sum_{k=1}^{q}\sum_{i=1}^{q} w_{kl}\langle J_i, J_k\rangle_F w_{ij} \\ &= \big(\Lambda_J^{-\frac{1}{2}} W_J^T \mathcal{X}_J W_J \Lambda_J^{-\frac{1}{2}}\big)_{l,j} = \delta_{lj}.\end{aligned}$$

∎

Having V_l, the functions $g_l(U_{a_1}\tilde{a}_1)$ are calculated from the condition that the selected components of the matrix $S_{\mathcal{K}}^T J_f(U_{a_1}\tilde{a}_1)$ and its approximation in (4.13) coincide, i.e.,

$$\big(S_{\mathcal{K}}^T J_f(U_{a_1}\tilde{a}_1)\big)_{i,j} = \Big(\sum_{l=1}^{p} V_l\, g_l(U_{a_1}\tilde{a}_1)\Big)_{i,j} = \sum_{l=1}^{p} \big(V_l\big)_{i,j}\, g_l(U_{a_1}\tilde{a}_1) \tag{4.17}$$

for some (i, j). Such components are determined successively from the basis matrices $V_1, \ldots, V_p$ using the MDEIM-Greedy procedure presented in Algorithm 4. This procedure is an generalization of the DEIM algorithm [11] to the matrix case.

Algorithm 4 MDEIM-Greedy procedure.

Input: $V_1, \ldots, V_p \in \mathbb{R}^{\ell, n_1}$.
Output: Set of indices $\mathcal{I} = \{(i_1, j_1), \ldots, (i_p, j_p)\}$.

1: Find $(i_1, j_1) = \underset{\substack{1 \le i \le \ell \\ 1 \le j \le n_1}}{\arg\max} |(V_1)_{i,j}|$.
2: $\mathcal{I} = \{(i_1, j_1)\}$, $G_1 = (V_1)_{i_1,j_1}$.
3: **for** $l = 2$ **to** p **do**
4: Set $b = \big[\,(V_l)_{i_1,j_1}, \ldots, (V_l)_{i_{l-1},j_{l-1}}\,\big]^T$.
5: Solve $G_{l-1}c = b$ for $c = [c_1, \ldots, c_{l-1}]^T$.
6: Compute $R_l = V_l - \sum_{k=1}^{l-1} V_k c_k$.
7: Find $(i_l, j_l) = \underset{\substack{1 \le i \le \ell \\ 1 \le j \le n_1}}{\arg\max} |(R_l)_{i,j}|$.
8: $\mathcal{I} \leftarrow \mathcal{I} \cup \{(i_l, j_l)\}$
9: $G_l = \begin{bmatrix} G_{l-1} & b \\ v & (V_l)_{i_l,j_l} \end{bmatrix}$ with $v = [\,(V_1)_{i_l,j_l}, \ldots, (V_{l-1})_{i_l,j_l}]$
10: **end for**

The following lemma shows that the matrix G_p in Algorithm 4 is nonsingular, and, hence, we get from (4.17) that

$$\begin{bmatrix} g_1(U_{a_1}\tilde{a}_1) \\ \vdots \\ g_p(U_{a_1}\tilde{a}_1) \end{bmatrix} = G_p^{-1}\vartheta(U_{a_1}\tilde{a}_1) \quad \text{with} \quad \vartheta(U_{a_1}\tilde{a}_1) = \begin{bmatrix} \big(S_{\mathcal{K}}^T J_f(U_{a_1}\tilde{a}_1)\big)_{i_1,j_1} \\ \vdots \\ \big(S_{\mathcal{K}}^T J_f(U_{a_1}\tilde{a}_1)\big)_{i_p,j_p} \end{bmatrix}.$$

LEMMA 4.2. *The matrices G_l, $l = 1, \ldots, p$, in Algorithm 4 are nonsingular.*

Proof. The result can be proved by induction. First, we note that $G_1 = (V_1)_{i_1,j_1} \neq 0$ for (i_1, j_1) as in Step 1 of Algorithm 4. This property immediately follows from $V_1 \neq 0$. Assume that G_{l-1} for $l > 1$ is nonsingular. Then using $b = G_{l-1}c$ we get

$$G_l \begin{bmatrix} I & -c \\ 0 & 1 \end{bmatrix} = \begin{bmatrix} G_{l-1} & 0 \\ v & (V_l)_{i_l,j_l} - vc \end{bmatrix}. \tag{4.18}$$

By Lemma 4.1, the matrices $V_1, \ldots, V_l$ are linear independent, and, hence, $R_l \neq 0$. This implies that $(V_l)_{i_l,j_l} - vc = (R_l)_{i_l,j_l} \neq 0$ for (i_l, j_l) as in Step 7 of Algorithm 4. Then the matrix in the right-hand side of (4.18) is nonsingular, and, thus, G_l is nonsingular too. □

Similar to the nonlinearity $f(U_{a_1}\tilde{a}_1)$ in (4.12), for the MDEIM index set $\mathcal{I} = \{(i_1, j_1), \ldots, (i_p, j_p)\}$, the vector-valued function $\vartheta(U_{a_1}\tilde{a}_1)$ depends only on a few components of $U_{a_1}\tilde{a}_1$ which are determined by an extended index set

$$\mathcal{I}_{ext} = \bigcup_{(i,j)\in\mathcal{I}} \left\{ l \in \{1, \ldots, n_1\} \ : \ \mathring{\operatorname{supp}}(\varphi_l) \cap \mathring{\operatorname{supp}}(\varphi_i) \cap \mathring{\operatorname{supp}}(\varphi_j) \neq \emptyset \right\}. \tag{4.19}$$

To emphasize the dependence on the selected components, we introduce a new function

$$\hat{\vartheta}(S_{\mathcal{I}_{ext}}^T U_{a_1}\tilde{a}_1) = \vartheta(U_{a_1}\tilde{a}_1), \tag{4.20}$$

where $S_{\mathcal{I}_{ext}}$ is the selector matrix associated with $\mathcal{I}_{ext}$.

An exemplary construction of the index sets $\mathcal{K}_{ext}$ and $\mathcal{I}_{ext}$ and the corresponding integration domains are presented in Figure 1.

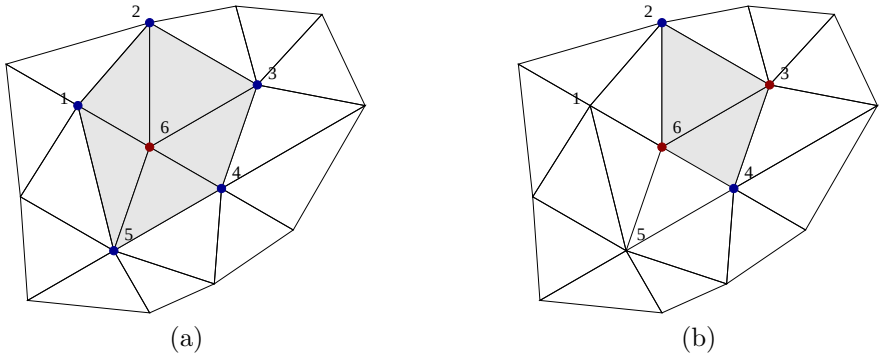

FIG. 1. *An example for the (extended) index sets and the integration domains:* (a) $\mathcal{K} = \{6\}$ *and* $\mathcal{K}_{ext} = \{1, 2, 3, 4, 5, 6\}$ *for a vector-valued function;* (b) $\mathcal{I} = \{(6, 3)\}$ *and* $\mathcal{I}_{ext} = \{2, 3, 4, 6\}$ *for a matrix-valued function.*

4.4. Offline-online decomposition. As it was mentioned above, the model reduction procedure and simulation of the resulting reduced-order model admit the decomposition into a computationally expensive offline stage and a rapid online stage. The offline stage includes the following steps:

1. Compute the snapshot matrices $\mathcal{X}_{a_1} = [a_1(t_1), \ldots, a_1(t_q)]$ and $\mathcal{X}_f$ as in (4.6).
2. Construct the POD projection matrices $U_{a_1} \in \mathbb{R}^{n_1, r_1}$ and $U_f \in \mathbb{R}^{n_1, \ell}$ from the SVDs (4.2) and (4.7), respectively.
3. Select the index set $\mathcal{K} = \{k_1, \ldots, k_\ell\}$ using DEIM applied to U_f. For all $k \in \mathcal{K}$, construct $\mathcal{K}_{ext,k}$ as in (4.11) and set $\mathcal{K}_{ext} = \bigcup_{k\in\mathcal{K}} \mathcal{K}_{ext,k}$.
4. Compute the snapshot matrix $\mathcal{X}_J$ as in (4.14) and construct the basis matrices $V_1, \ldots, V_p \in \mathbb{R}^{\ell, n_1}$ as in (4.16) using the EVD (4.15).
5. Select the index set $\mathcal{I} = \{(i_1, j_1), \ldots, (i_p, j_p)\}$ using MDEIM applied to the matrices $V_1, \ldots, V_p$ and construct $\mathcal{I}_{ext}$ as in (4.19).

6. Compute and store the time-independent matrices
$\tilde{E}_1 = U^T E_1 U \in \mathbb{R}^{r_1+m,\, r_1+m}$,
$\tilde{B}_1 = U^T B_1 \in \mathbb{R}^{r_1+m,m}$, $\tilde{C}_1 = C_1 U \in \mathbb{R}^{m,r_1+m}$,
$\tilde{A}_l = U^T A_l U \in \mathbb{R}^{r_1+m,r_1+m}$ with U as in (4.4),
$W = U_{a_1}^T U_f (S_{\mathcal{K}}^T U_f)^{-1} \in \mathbb{R}^{r_1,\ell}$ with $S_{\mathcal{K}} = [e_{k_1}, \ldots, e_{k_\ell}]$,
$U_{\mathcal{K}_{ext}} = S_{\mathcal{K}_{ext}}^T U_{a_1} \in \mathbb{R}^{|\mathcal{K}_{ext}|, r_1}$ with the selector matrix $S_{\mathcal{K}_{ext}}$ associated with $\mathcal{K}_{ext}$,
$\tilde{V}_i = W V_i U_{a_1} \in \mathbb{R}^{r_1,\, r_1}$ for $i = 1, \ldots, p$,
$U_{\mathcal{I}_{ext}} = S_{\mathcal{I}_{ext}}^T U_{a_1} \in \mathbb{R}^{|\mathcal{I}_{ext}|,\, r_1}$ with the selector matrix $S_{\mathcal{I}_{ext}}$ associated with $\mathcal{I}_{ext}$,
$G_p = \begin{bmatrix} (V_1)_{i_1,j_1} & \cdots & (V_p)_{i_1,j_1} \\ \vdots & \ddots & \vdots \\ (V_1)_{i_p,j_p} & \cdots & (V_p)_{i_p,j_p} \end{bmatrix} \in \mathbb{R}^{p,p}$.

Then in the online stage, we solve the POD-DEIM reduced-order model

$$\begin{aligned} \tilde{E}_1 \dot{\tilde{x}}_1 &= \tilde{f}_1(\tilde{x}_1) + \tilde{B}_1 u, \\ \tilde{y} &= \tilde{C}_1 \tilde{x}_1, \end{aligned}$$

where

$$\tilde{x}_1 = \begin{bmatrix} \tilde{a}_1 \\ \tilde{a}_{21} \end{bmatrix}, \qquad \tilde{f}_1(\tilde{x}_1) = \tilde{A}_l \tilde{x}_1 + \begin{bmatrix} W \hat{f}(U_{\mathcal{K}_{ext}} \tilde{a}_1) \\ 0 \end{bmatrix},$$

and $\hat{f}$ is as in (4.12). The approximate Jacobi matrix of $\tilde{f}_1$ at $\tilde{x}_1$ is given by

$$\tilde{J}_{\tilde{f}_1}(\tilde{x}_1) = \tilde{A}_l + \begin{bmatrix} \sum_{l=1}^{p} \tilde{V}_i \, \tilde{g}_i(\tilde{a}_1) \\ 0 \end{bmatrix} \quad \text{with} \quad \begin{bmatrix} \tilde{g}_1(\tilde{a}_1) \\ \vdots \\ \tilde{g}_p(\tilde{a}_1) \end{bmatrix} = G_p^{-1} \hat{\vartheta}(U_{\mathcal{I}_{ext}} \tilde{a}_1),$$

where $\hat{\vartheta}$ is as in (4.20). One can see that all computations in this stage do not depend on the original dimension $n_a + m$ that significantly reduces the computational cost.

5. Numerical experiments. In this section, we present some results of numerical experiments for model reduction of linear and nonlinear MQS models describing a single-phase 2D transformer with an iron core and two coils as shown in Figure 2, see [36] for detailed description and geometry data.

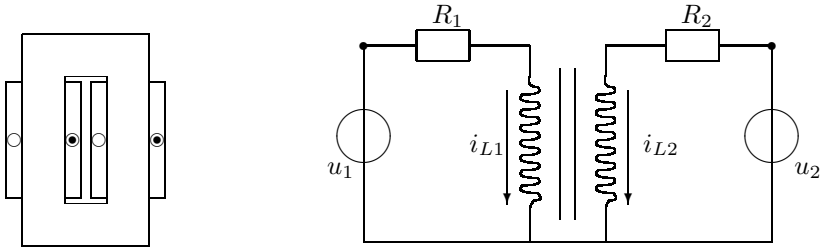

FIG. 2. *Single-phase 2D transformer and transformer equivalent circuit.*

For the FEM discretization, we use the free available software FEniCS*, whereas the time integration is done by the solver IDA from the simulation package Assimulo†.

*http://fenicsproject.org
†http://www.jmodelica.org/assimulo

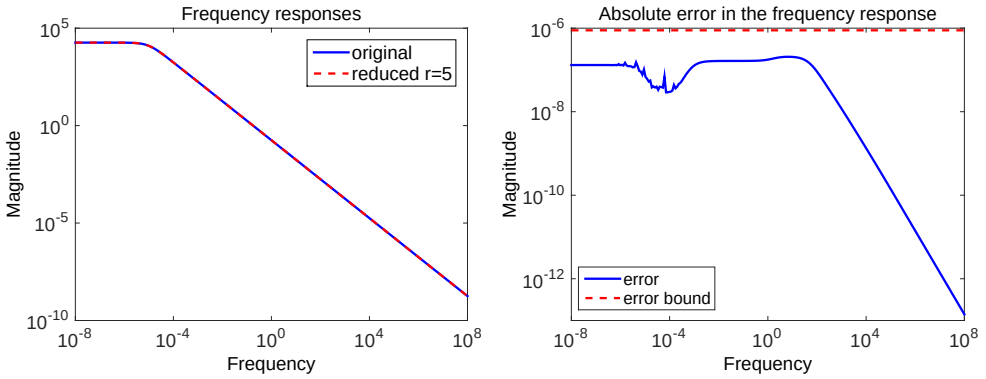

(a) (b)

FIG. 3. *Linear MQS model:* (a) *the frequency responses of the original and reduced-order models;* (b) *the absolute error in the frequency domain and the error bound* γ.

The dimensions of the spatially discretized MQS system are $n_a = 17731$, $n_1 = 7200$, $n_2 = 10531$ and $m = 2$. We choose the material parameters $\sigma_1 = 5 \cdot 10^5\,\Omega^{-1}\mathrm{m}^{-1}$ and $\nu_2 = 1\,\mathrm{AmV}^{-1}\mathrm{s}^{-1}$. Furthermore, we take $\nu_1 = 14872\,\mathrm{AmV}^{-1}\mathrm{s}^{-1}$ for the linear model and $\nu_1(\eta) = 3.8\,\exp(2.14\eta) + 396.2\,\mathrm{AmV}^{-1}\mathrm{s}^{-1}$ for the nonlinear system.

Example 1. First, we apply the balanced truncation model reduction method to the linear transformer model as described in Section 3. The controllability Gramian P was approximated by a low-rank matrix $P \approx \tilde{Z}_{\tilde{n}}\tilde{Z}_{\tilde{n}}^T$ with $Z_{\tilde{n}} \in \mathbb{R}^{n,\tilde{n}}$ computed by the LR-ADI method (3.15). Here, $n = 7202$ and $\tilde{n} = 36$. The resulting Hankel singular values decay very rapidly implying that the MQS system can be well approximated by a model of low dimension r. We approximate the original system by a reduced model of order $r = 5$. Figure 3(a) shows the spectral norms of the frequency responses $\|H(\mathrm{i}\omega)\|_2$ and $\|\tilde{H}(\mathrm{i}\omega)\|_2$ of the full and reduced-order models for $\omega \in [10^{-8}, 10^8]$. In Figure 3(b), we present the absolute error in the frequency domain given by $\|H(\mathrm{i}\omega) - \tilde{H}(\mathrm{i}\omega)\|_2$ and the error bound computed as

$$\gamma = 2(\sigma_{r+1} + \ldots + \sigma_{\tilde{n}-1} + (n - \tilde{n} + 1)\sigma_{\tilde{n}}) = 8.967 \cdot 10^{-7}.$$

Figure 4(a) shows the components of the output vectors $y(t) = [y_1(t), y_2(t)]^T$ and $\tilde{y}(t) = [\tilde{y}_1(t), \tilde{y}_2(t)]^T$ of the original and reduced-order models, respectively, on the time interval $[0, 0.01]s$ resulting for the input

$$u(t) = \begin{bmatrix} 45.5 \cdot 10^3 \sin(900\pi t) \\ 77 \cdot 10^3 \sin(1700\pi t) \end{bmatrix}.$$

The relative error $\|y(t) - \tilde{y}(t)\|/\|y(t)\|$ in the output is presented in Figure 4(b). One can see that the errors in the frequency and time domains are both small.

Example 2. In the second example, we examine model reduction of the nonlinear transformer model using the POD-DEIM-MDEIM method. The snapshots were collected for the training input $u(t)$ and the reduced-order model was then tested for the input $u_{\mathrm{test}}(t)$ given by

$$u(t) = \begin{bmatrix} 45.5 \cdot 10^3 \sin(900\pi t) \\ 77 \cdot 10^3 \sin(1700\pi t) \end{bmatrix}, \qquad u_{\mathrm{test}}(t) = \begin{bmatrix} 46.5 \cdot 10^3 \sin(1500\pi t) \\ 78 \cdot 10^3 \sin(1000\pi t) \end{bmatrix}.$$

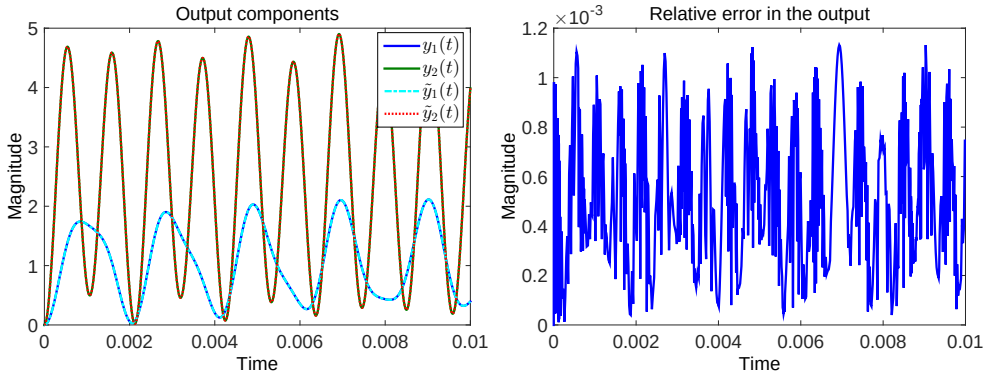

FIG. 4. *Linear MQS model:* (a) *The output components of the original and reduced-order models;* (b) *the relative error in the output.*

Figure 5 shows the singular values σ_j^{POD} and σ_j^{DEIM} of the POD and DEIM snapshot matrices $\mathcal{X}_{a_1}$ and $\mathcal{X}_f$, respectively, as well as the eigenvalues $\lambda_j^{\mathrm{MDEIM}}$ of the MDEIM snapshot matrix $\mathcal{X}_J$. We assume that the singular values and the eigenvalues are ordered decreasingly. Based on these values, the reduced dimensions were chosen as

$$\text{POD: } r_1 = 38, \qquad \text{DEIM: } \ell = 3, \qquad \text{MDEIM: } p = 3$$

with the relations

$$\frac{\sigma_{39}^{\mathrm{POD}}}{\sigma_1^{\mathrm{POD}}} = 10^{-7}, \qquad \frac{\sigma_4^{\mathrm{DEIM}}}{\sigma_1^{\mathrm{DEIM}}} = 2.8 \cdot 10^{-2}, \qquad \frac{\lambda_4^{\mathrm{MDEIM}}}{\lambda_1^{\mathrm{MDEIM}}} = 2.1 \cdot 10^{-6}.$$

The reduced model has the dimension $r = r_1 + m = 40$. Note that the matrix $S_{\mathcal{K}}^T J_f \in \mathbb{R}^{3,7200}$ has only 19 nonzero entries. Using the MDEIM method, this dimension can further be reduced resulting in evaluation of 3 entries only. The extended index sets $\mathcal{K}_{ext}$ and $\mathcal{I}_{ext}$ have $|\mathcal{K}_{ext}| = 17$ and $|\mathcal{I}_{ext}| = 14$ elements.

In Figure 6(a), we present the output components of the original and POD-DEIM-MDEIM-reduced models, whereas the relative errors

$$\frac{\|y(t) - \tilde{y}(t)\|}{\max\limits_{t\in[0,0.01]} \|y(t)\|}$$

for the POD-, POD-DEIM- and POD-DEIM-MDEIM-reduced models are given in Figure 6(b). We observe that the errors are about the same for all three reduced models meaning that the errors introduced by DEIM and MDEIM are negligible compared to the POD error.

6. Conclusion. In this paper, we have considered model order reduction of linear and nonlinear MQS systems arising in electromagnetic simulations. The FEM discretization of the underlying Maxwell's equation leads to a DAE system of index one with a very special block structure. Our model reduction approach is based on transforming the DAE system into the ODE form by eliminating the algebraic components and reducing the differential components only. For model reduction of the linear MQS system, we have used a balanced truncation method. It was shown

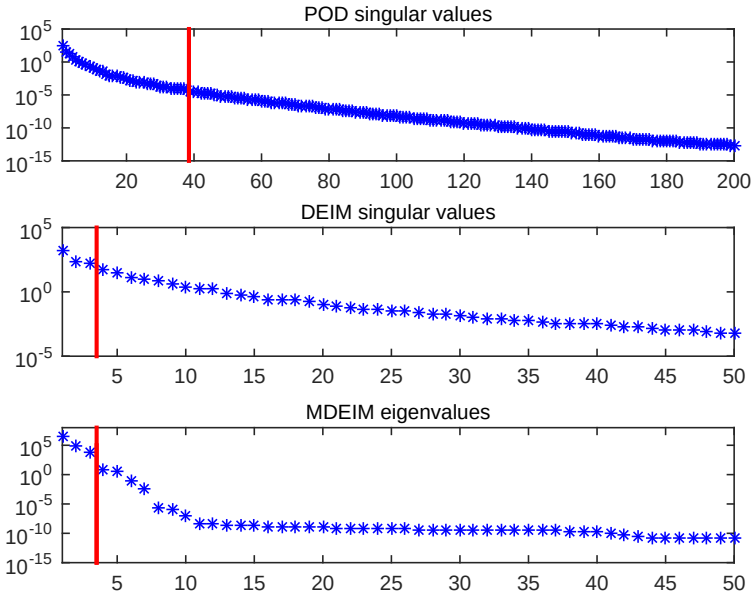

FIG. 5. *Nonlinear MQS model:* (a) *POD singular values;* (b) *DEIM singular values;* (c) *MDEIM eigenvalues.*

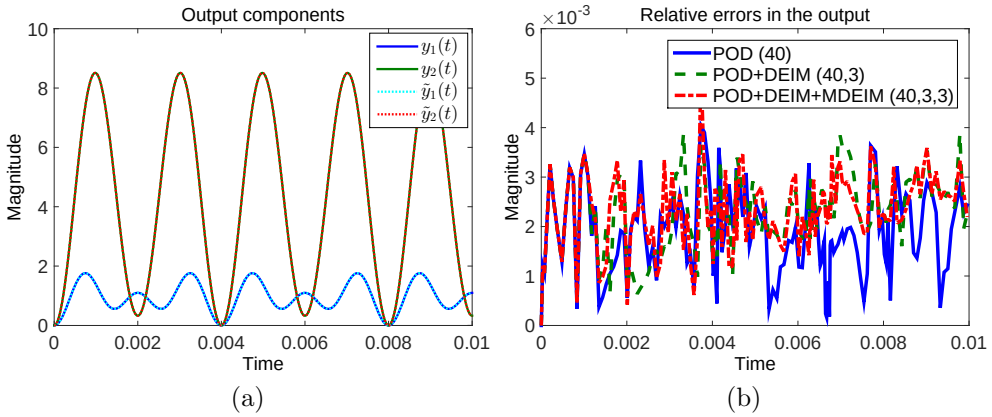

FIG. 6. *Nonlinear MQS model:* (a) *the output components of the original and reduced-order models;* (b) *the relative errors in the output.*

that under certain symmetry conditions the linear MQS system is passive and the Lyapunov-based balanced truncation method preserves passivity in the reduced-order model. The nonlinear MQS system was approximated by the POD method combined with DEIM and MDEIM. For fast evaluation of the Jacobi matrix, we have presented an efficient modification of MDEIM which avoids the vectorization of the snapshot matrix.

Acknowledgments. The authors would like to thank Sebastian Schöps for helpful discussions.

REFERENCES

[1] B.D.O. Anderson and S. Vongpanitlerd, *Network Analysis and Synthesis*, Prentice Hall, Englewood Cliffs, NJ, 1973.

[2] A. Bartel, S. Baumanns, and S. Schöps, *Structural analysis of electrical circuits including magnetoquasistatic devices*, Appl. Numer. Math., 61 (2011), pp. 1257–1270.

[3] P. Benner and M.W. Hess, *A reduced basis method for microwave semiconductor devices with geometric variations*, COMPEL, 33 (2014), pp. 1071–1081.

[4] P. Benner, P. Kürschner, and J. Saak, *Efficient handling of complex shift parameters in the low-rank Cholesky factor ADI method*, Numer. Algorithms, 62 (2013), pp. 225–251.

[5] P. Benner, P. Kürschner, and J. Saak, *An improved numerical method for balanced truncation for symmetric second-order systems*, Math. Comput. Model. Dyn. Systems, 19 (2013), pp. 593–615.

[6] ———, *Self-generating and efficient shift parameters in ADI methods for large Lyapunov and Sylvester equations*, Electron. Trans. Numer. Anal., 43 (2014), pp. 142–162.

[7] P. Benner and T. Stykel, *Model reduction of differential-algebraic equations: a survey*, in Surveys in Differential-Algebraic Equations IV, A. Ilchmann and T. Reis, eds., Differential-Algebraic Equations Forum, Springer-Verlag, to appear.

[8] A. Bodendiek and M. Bollhöfer, *Adaptive-order rational Arnoldi-type methods in computational electromagnetism*, BIT Numer. Math., 54 (2014), pp. 357–380.

[9] R.-U. Börner, O.G. Ernst, and K. Spitzer, *Fast 3-D simulation of transient electromagnetic fields by model reduction in the frequency domain using Krylov subspace projection*, Geophys. J. Int., 173 (2008), pp. 766–780.

[10] K.E. Brenan, S.L. Campbell, and L.R. Petzold, *The Numerical Solution of Initial-Value Problems in Differential-Algebraic Equations*, Classics in Applied Mathematics, 14, SIAM, Philadelphia, PA, 1996.

[11] S. Chaturantabut and D.C. Sorensen, *Nonlinear model reduction via discrete empirical interpolation*, SIAM J. Sci. Comput., 32 (2010), pp. 2737–2764.

[12] Y. Chen, J.S. Hesthaven, and Y. Maday, *A seamless reduced basis element method for 2D Maxwell's problem: an introduction*, in Spectral and High Order Methods for Partial Differential Equations, J.S. Hesthaven and E.M. Rønnquist, eds., vol. 76 of Lecture Notes in Computational Science and Engineering, Springer-Verlag, Berlin, Heidelberg, 2011, pp. 141–152.

[13] F.D. Freitas, J. Rommes, and N. Martins, *Gramian-based reduction method applied to large sparse power system descriptor models*, IEEE Trans. Power Systems, 23 (2008), pp. 1258–1270.

[14] K. Glover, *All optimal Hankel-norm approximations of linear multivariable systems and their L^∞-error bounds*, Internat. J. Control, 39 (1984), pp. 1115–1193.

[15] E. Hairer, S.P. Nørsett, and G. Wanner, *Solving Ordinary Differential Equations I - Non-stiff Problems*, vol. 8 of Springer Series in Computational Mathematics, Springer-Verlag, Berlin, Heidelberg, 1993.

[16] M. Heinkenschloss, D.C. Sorensen, and K. Sun, *Balanced truncation model reduction for a class of descriptor systems with application to the Oseen equations*, SIAM J. Sci. Comp., 30 (2008), pp. 1038–1063.

[17] T. Henneron and S. Clénet, *Model order reduction of quasi-static problems based on POD and PGD approaches*, Eur. Phys. J. Appl. Phys., 64 (2013), pp. 24514:p1–p7.

[18] ———, *Model order reduction of non-linear magnetostatic problems based on POD and DEI methods*, IEEE Trans. Magn., 50 (2014), pp. 33–36.

[19] R. Hiptmair, *Multilevel gauging for edge elements*, Computing, 64 (2000), pp. 97–122.

[20] R.A. Horn and F. Zhang, *Basic properties of the Schur complement*, in The Schur Complement and Its Applications, F. Zhang, ed., vol. 4 of Numerical Methods and Algorithms, Springer-Verlag, Berlin, Heidelberg, 2005, pp. 17–46.

[21] L. Jansen, U. Römer, and S. Schöps, *Abstract differential-algebraic equations in low-frequency electrical engineering*. Talk at the GAMM Annual Meeting 2014, Erlangen, March 10–14, 2014.

[22] P. Kunkel and V. Mehrmann, *Differential-Algebraic Equations. Analysis and Numerical Solution*, EMS Publishing House, Zürich, Switzerland, 2006.

[23] R. Lamour, R. März, and C. Tischendorf, *Differential-Algebraic Equations: A Projector Based Analysis*, Differential-Algebraic Equations Forum, Springer-Verlag, Berlin, Heidelberg, 2013.

[24] J.-R. Li and J. White, *Low rank solution of Lyapunov equations*, SIAM J. Matrix Anal. Appl., 24 (2002), pp. 260–280.

[25] J.B. Manges and Z.J. Cendes, *A generalized tree-cotree gauge for magnetic field computation*,

IEEE Trans. Magnetics, 31 (1995), pp. 1342–1347.

[26] V. Mehrmann, *Index concepts for differential-algebraic equations*, Preprint 3-2012, Technische Universität Berlin, 2012. To appear in Encyclopedia of Applied and Computational Mathematics, Springer-Verlag, Berlin, 2016.

[27] P. Monk, *Finite Element Methods for Maxwell's Equations*, Numerical mathematics and scientific computation, Oxford University Press, 2003.

[28] B.C. Moore, *Principal component analysis in linear systems: controllability, observability, and model reduction*, IEEE Trans. Automat. Control, AC-26 (1981), pp. 17–32.

[29] J.C. Nédélec, *Mixed finite elements in R^3*, Numer. Math., 35 (1980), pp. 315–341.

[30] S. Nicaise and F. Tröltzsch, *A coupled Maxwell integrodifferential model for magnetization processes*, Math. Nachr., 287 (2014), pp. 432–452.

[31] S. Nicaise, S. Stingelin and F. Tröltzsch, *On two optimal control problems for magnetic fields*, Comput. Methods Appl. Math., 14 (2014), pp. 555–573.

[32] T. Penzl, *A cyclic low-rank Smith method for large sparse Lyapunov equations*, SIAM J. Sci. Comp., 21 (1999/2000), pp. 1401–1418.

[33] J. Pomplun, *Reduced basis method for electromagnetic scattering problems*, Ph.D. thesis, Free University Berlin, 2010.

[34] Y. Sato, M. Clemens, and H. Igarashi, *Adaptive subdomain model order reduction with discrete empirical interpolation method for nonlinear magneto-quasi-static problems*, in Proceedings of the 20th International Conference on the Computation of Electromagnetic Fields (COMPUMAG 2015), Montreal, Canada, June 28 - July 02, 2015.

[35] D. Schmidthäusler, S. Schöps, and M. Clemens, *Linear subspace reduction for quasistatic field simulations to accelerate repeated computations*, IEEE Trans. Magn., 50 (2014), p. 7010304.

[36] S. Schöps, *Multiscale Modeling and Multirate Time-Integration of Field/Circuit Coupled Problems*, Ph.D. thesis, Bergische Universität Wuppertal, 2011.

[37] S. Schöps, H. De Gersem, and T. Weiland, *Winding functions in transient magnetoquasistatic field-circuit coupled simulations*, COMPEL, 32 (2013), pp. 2063–2083.

[38] L. Sirovich, *Turbulence and the dynamics of coherent structures: parts i-iii*, Quart. Appl. Math., 45 (1987), pp. 561–590.

[39] R. Stefanescu and A. Sandu, *Efficient approximation of sparse jacobians for time-implicit reduced order models*, arxiv:1409.5506v3, 2015.

[40] T. Stykel, *Gramian-based model reduction for descriptor systems*, Math. Control Signals Systems, 16 (2004), pp. 297–319.

[41] ———, *Balancing-related model reduction of circuit equations using topological structure*, in Model Reduction for Circuit Simulation, P. Benner, M. Hinze, and E.J.W ter Maten, eds., vol. 74 of Lecture Notes in Electrical Engineering, Springer-Verlag, Berlin, Heidelberg, 2011, pp. 53–80.

[42] T. Stykel and C. Willbold, *Model reduction based optimal control for field-flow fractionation*, in Proceedings of the GAMM Annual Meeting (GAMM 2013, Novi Sad, March 18-22, 2013), 2013.

[43] M.M. Uddin, J. Saak, B. Kranz, and P. Benner, *Computation of a compact state space model for an adaptive spindle head configuration with piezo actuators using balanced truncation*, Prod. Eng. Res. Devel., 6 (2012), pp. 577–586.

[44] S. Volkwein, *Proper Orthogonal Decomposition: Theory and Reduced-Order Modelling*, Lecture Notes, University of Konstanz, Konstanz, 2013.

[45] T. Weiland, *A discretization method for the solution of Maxwell's equations for six-component fields*, Electron. Commun., 31 (1977), pp. 116–120.

[46] D. Wirtz, D.C. Sorensen, and B. Haasdonk, *A posteriori error estimation for DEIM reduced nonlinear dynamical systems*, SIAM J. Sci. Comput., 36 (2014), pp. A311–A338.

[47] T. Witting, R. Schuhmann, and T. Weiland, *Model order reduction for large systems in computational electromagnetics*, Linear Algebra Appl., 415 (2006), pp. 499–530.